Metadata of the chapter that will be visualized online

Chapter Title	Remote Sensing Technologies for the Assessment of Marine and Coastal Ecosystems	
Copyright Year	2016	
Copyright Holder	Springer International Publishing Switzerland	
Corresponding Author	Family Name	**Gutierres**
	Particle	
	Given Name	**Francisco**
	Suffix	
	Division	Institute of Geography and Spatial Planning
	Organization/University	University of Lisbon
	Street	Edifício IGOT, Avenida Prof. Gama Pinto
	Postcode	1600-214
	City	Lisbon
	Country	Portugal
	Email	franciscogutierres@campus.ul.pt
Author	Family Name	**Teodoro**
	Particle	
	Given Name	**Ana Cláudia**
	Suffix	
	Division	Earth Sciences Institute (ICT) and Department of Geosciences, Environment and Land Planning, Faculty of Sciences
	Organization/University	University of Porto
	Street	Rua do Campo Alegre
	Postcode	4169-007
	City	Porto
	Country	Portugal
	Email	amteodor@fc.up.pt

Author	Family Name	**Reis**
	Particle	
	Given Name	**Eusébio**
	Suffix	
	Division	Institute of Geography and Spatial Planning
	Organization/University	University of Lisbon
	Street	Edifício IGOT, Avenida Prof. Gama Pinto
	Postcode	1600-214
	City	Lisbon
	Country	Portugal
	Email	eusebioreis@campus.ul.pt
Author	Family Name	**Neto**
	Particle	
	Given Name	**Carlos**
	Suffix	
	Division	Institute of Geography and Spatial Planning
	Organization/University	University of Lisbon
	Street	Edifício IGOT, Avenida Prof. Gama Pinto
	Postcode	1600-214
	City	Lisbon
	Country	Portugal
	Email	cneto@campus.ul.pt
Author	Family Name	**Costa**
	Particle	
	Given Name	**José Carlos**
	Suffix	
	Division	Higher Institute of Agronomy
	Organization/University	University of Lisbon
	Street	Tapada da Ajuda
	Postcode	1349-017

	City	Lisbon
	Country	Portugal
	Email	jccosta@isa.ulisboa.pt

Abstract	This chapter reviews the Remote Sensing (RS) technologies that are particularly appropriate for marine and coastal ecosystem research and management. RS techniques are used to perform analysis of water quality in coastal water bodies; to identify, characterize and analyze river plumes; to extract estuarine/coastal sandy bodies; to identify beach features/patterns; and to evaluate the changes and integrity (health) of the coastal lagoon habitats. For effective management of these ecosystems, it is essential to have satellite data available and complementary accurate information about the current state of the coastal regions, in addition to well-informed forecasts about its future state. In recent years, the use of space, air and ground-based RS strategies has allowed for the rapid data collection, Image processing (Pixel-Based and Object-Based Image Analysis (OBIA) classification) and dissemination of such information to reduce vulnerability to natural hazards, anthropic pressures, and to monitoring essential ecological processes, life support systems and biological diversity. Q1

AUTHOR QUERIES

Q1 Please check captured abstract if correct.

3 Remote Sensing Technologies for the Assessment of Marine and Coastal Ecosystems

Francisco Gutierres, Ana Cláudia Teodoro, Eusébio Reis, Carlos Neto, and José Carlos Costa

Abstract

This chapter reviews the Remote Sensing (RS) technologies that are particularly appropriate for marine and coastal ecosystem research and management. RS techniques are used to perform analysis of water quality in coastal water bodies; to identify, characterize and analyze river plumes; to extract estuarine/coastal sandy bodies; to identify beach features/patterns; and to evaluate the changes and integrity (health) of the coastal lagoon habitats. For effective management of these ecosystems, it is essential to have satellite data available and complementary accurate information about the current state of the coastal regions, in addition to well-informed forecasts about its future state. In recent years, the use of space, air and ground-based RS strategies has allowed for the rapid data collection, Image processing (Pixel-Based and Object-Based Image Analysis (OBIA) classification) and dissemination of such information to reduce vulnerability to natural hazards, anthropic pressures, and to monitoring essential ecological processes, life support systems and biological diversity.

F. Gutierres (✉) • E. Reis • C. Neto
Institute of Geography and Spatial Planning,
University of Lisbon, Edifício IGOT,
Avenida Prof. Gama Pinto, 1600-214
Lisbon, Portugal
e-mail: franciscogutierres@campus.ul.pt;
eusebioreis@campus.ul.pt; cneto@campus.ul.pt

A.C. Teodoro
Earth Sciences Institute (ICT) and Department of
Geosciences, Environment and Land Planning,
Faculty of Sciences, University of Porto,
Rua do Campo Alegre, 4169-007 Porto, Portugal
e-mail: amteodor@fc.up.pt

J.C. Costa
Higher Institute of Agronomy, University of Lisbon,
Tapada da Ajuda, 1349-017 Lisbon, Portugal
e-mail: jccosta@isa.ulisboa.pt

C.W. Finkl, C. Makowski (eds.), *Seafloor Mapping along Continental Shelves*,
Coastal Research Library 13, DOI 10.1007/978-3-319-25121-9_3

3.1 Introduction

The coastal areas are zones of primary importance from human and ecological perspectives. Nearly all of the maritime resource is on a narrow continental shelf which is affected by ecological pressures owing to a large-scale population increase in the coastal areas (half of the world's population lives at least 60 km from a coast, and the proportion will be 70 % in 2020) (FAO 2014).

In recent years, a number of RS are available to resource managers for developing effective marine ecosystem management initiatives, including the use of information technology for analyzing and understanding an ecosystem as a whole and not simply the targeted resource or a specific area.

The wide applicability of RS techniques has allowed researchers and managers to take a broader view of coastal ecosystem assessment and management (Klemas 2011; Yang 2009). Ecological patterns, processes and changes in composition and structure of coastal ecosystems can be quantified using satellite imagery. When these RS tools for generating, organizing, storing, and analyzing spatial information are combined with mathematical and data mining models, marine resource planners and managers have the means for accessing the impacts of natural events, anthropic and alternative management practices on pattern and process on coastal areas.

RS provide not only photographic representation of the coastal and marine surfaces, but also physical (absorbency, reflectance and emissivity) measurements of various properties of these ecosystems. These spectral characteristics can be used to access the major factors affecting water quality in coastal water bodies (e.g. Total Suspended Matter (TSM) and dissolved organic matter (DOM)) (Vanhellemont and Ruddick 2014; Tang et al. 2013; Zhu et al. 2013, 2014; Liew et al. 2011; Vantrepotte et al. 2011; Nechad et al. 2010; Rodríguez-Guzmán and Gilbes-Santaella 2009; Wang 2009; Teodoro et al. 2007a, b; Zhou et al. 2006; Bustamante et al. 2006; Ruddick et al. 2003); to identify, characterize and analyze river plumes (Mendes et al. 2014; Guneroglu et al. 2013; Gonçalves et al. 2012; Rudorff et al. 2011; Teodoro et al. 2009a; Otero et al. 2008); to extract estuarine/coastal sandy bodies (Teodoro and Gonçalves 2012; Chowdhury et al. 2011; Teodoro et al. 2011a, b; Silveira and Heleno 2009; Baptista et al. 2008); to identify beach features/patterns (Teodoro 2015; Teodoro et al. 2009b, 2010, 2011b, c, 2013; Mujabar and Chandrasekar 2012; Harris et al. 2011; Pais-Barbosa et al. 2009); and to evaluate the changes and integrity (health) of the coastal lagoon habitats (Gutierres 2014; McCarthy and Halls 2014; Bustamante et al. 2013; Vahtmäe and Kutser 2013; Urbański 2009; Kutser et al. 2006; Druon et al. 2004; Sousa et al. 2003, 2010, 2013; Kandus et al. 1999), at various scales. In fact, the RS creates new opportunities for identifying which parameters function as regulators of marine/costal ecosystems activity at local and regional levels and how these variables differ across spatial and temporal scales.

Within the above context, this chapter is dedicated to the development of RS for monitoring, synthesis and modeling in the Portuguese coastal environment. Specifically, this chapter concentrates on the following aspects:

- Reviews the types of satellite imagery and RS methods applied in the marine/coastal environment management; and
- Examines some latest development in the use of RS for marine/coastal ecosystem assessment with emphasis on estuaries and coastal zones, shorelines and coastal wetlands.

In addition to scientific research, the chapter has incorporated a management component that can be found in six case studies, discussing our understanding of the status, trends and threats in coastal ecosystems. The sections below describe in more detail the conceptual and technical issues of applying RS techniques in coastal environments; and the major findings of different research projects related to the development of [AU2] RS techniques to identify ocean physical, optical, biological changes and coastal wetlands, using spectral and temporal signatures, supervised and unsupervised classification algorithms (pixel-based or object-based) and data mining models.

3.2 Status and Improvements for Assessment of Marine and Coastal Ecosystems

3.2.1 Remotely Sensed Data

Today, and given the numerous RS satellite imaging systems available, it is a challenge to choose the most appropriate satellite images for observing marine/coastal ecosystems – for technical details of the classification of remote sensors, readers can refer to see Klemas (2011). The digital systems can be grouped into four different types of resolution: spatial, spectral, radiometric, and temporal. The RS requirements for Open Ocean, Estuaries/Coastal lagoons and Land are presented in Table 3.1 (Klemas 2011). A list of the more relevant satellite sensors to the assessment of marine ecosystems is shown in Table 3.2, where several multispectral images can be used for mapping concentrations of organic/inorganic suspended particles, dissolved substances in coastal waters; coastal features and patterns and for others applications (Teodoro and Gonçalves 2011).

We highlighted some RS data that can be used in studies of marine/coastal ecosystems. Depending on the research to carry out it is important to consider the temporal or spatial characteristics of the RS satellite imagery used in each analysis. In the work developed by Teodoro et al. (2009a) and Teodoro and Gonçalves (2011), it was used the TSM concentration retrieved from MERIS scene, which allowed the extraction of objects corresponding to river plumes. The medium spatial resolution of MERIS data is enough to estimate the river plume size. MODIS has been providing atmospherically operational products since 2000 (Terra) and 2002 (Aqua) with different temporal frequencies. Moreover, the high temporal of MERIS data seems to be essential in monitoring river plume, subject to rapid changes due to extreme situations (e.g. precipitation, floods). According the same authors, the high spatial resolution of IKONOS-2 data seems to be a crucial factor in the sand spit area estimation.

Bustamante et al. (2013) based on MODIS provides the most coherent data record at moderate spatial resolution to study wetland dynamics included in the Spanish Ramsar Site Doñana, while LANDSAT family sensors (Multispectral Scanner – MSS, Thematic Mapper – TM, Enhanced Thematic Mapper Plus – ETM+ and Operational Land Imager – OLI) have the longest temporal coverage (>30 years) with a higher spatial resolution (30–90 m) but lower temporal frequency (16 days) (see Roy et al. 2014).

Gutierres (2014) showed that LANDSAT sensor has been an effective source for land cover data (see Fig. 3.1). Its 30 m resolution and spectral bands have proved adequate for observing land cover changes in coastal lagoons on the Portuguese southwest coast. Figure 3.2 shows a land cover map of the Site of Community Importance (SCI) of the Sado Estuary derived from a LANDSAT-7 ETM+ image containing 13 vegetation units (two wetland and three water classes), and also agricultural and urban classes.

Other similar satellites with medium-resolution imagers, such as SPOT-4/5 can also be used for change detection in water and wetland environment. However, finer details such as wetland habitats and species cannot be reliably differentiated at these resolutions. In this sense, several progresses is being made using high resolution sensors (GeoEye-1 and WorldView-2), with spatial resolutions of 0.5–1 m. These sensors have consistently demonstrated the ability to classify features at detailed levels. Thus Worldview-2 improves the segmentation and classification of land and aquatic features beyond any other space-based RS platform. According to Digital Globe (2010), the classification of water bodies is expected to improve from 85 to 90 % with traditional VNIR imagery (GeoEye-1 and similar) to between 95 and 98 % with Worldview-2. Also the bathymetric measurements are substantially improved in depth and accuracy with the introduction of the Coastal Blue band (440–450 m); the addition of the Red-Edge spectral band improve the accuracy and sensitivity of wetland plant studies; and the eight spectral bands and GSD are able to reveal significantly more detail in the spectral changes of

small ground features. These findings suggest that while traditional VNIR multispectral imagery is very capable at classifying water types, the additional spectral bands of WordView-2 provides an incremental improvement in feature classification applications.

Also conventional color satellites sensors such as SeaWIFS and MODIS have proven to be useful in retrieving water quality parameters in ocean waters (Liew et al. 2011). However, such sensors usually are low resolution, of about 1 km. This implies they are not suitable for inland and coastal waters due to land contamination. As previously discussed it is also important the use of high resolution satellite sensors to monitor the water quality of the ecosystems. In comparison to the conventional high resolution satellites such as LANDSAT, SPOT and IKONOS, the additional

t1.1 **Table 3.1** RS requirements for ocean, estuarine/coastal lagoons and land environments (Adapted from Klemas 2011)

t1.2		Open ocean	Estuaries/coastal lagoons	Land surface
t1.3	Spatial resolution	1–10 km	20–200 m	1–30 m
t1.4	Coverage area	2,000 × 2,000 km	200 × 200 km	200 × 200 km
t1.5	Frequency of coverage	1–6 days	0.5–6 h	0.5–5 years
t1.6	Dynamic range	Narrow	Wide	Wide
t1.7	Radiometric resolution	10–12 bits	10–12 bits	8–10 bits
t1.8	Spectral Resolution	Multispectral	Hyperspectral	Multispectral (hyperspectral)

t2.1 **Table 3.2** Characteristics of some current satellite RS systems (Adapted from Klemas 2011)

t2.2 t2.3	Satellite/sensor	Spectral range	Bands	GSD	Revisit time	Swath width	Application
t2.4 t2.5	AVHRR NOAA 15/16	580–12,500 nm	6	1.1 km	−12 h	2,400 km	SST, turbidity, circulation
t2.6	SeaWIFS	402–885 nm	8	1.1 km	daily	2,800 km	Ocean color, red products
t2.7 t2.8 t2.9	MODIS Terra/ Aqua	620–14,385 nm	16VNIR 4SWIR 16TIR	250 m–1 km	daily	2,330 km	SST, turbidity, circulation, ocean color
t2.10 t2.11	MISR Terra (9 camera angles)	425–886 nm	4	275 m	9 days	360 km	Ocean color, circulation
t2.12 t2.13 t2.14 t2.15	ASTER Terra	520–11,650 nm	3VNIR 6SWIR 5TIR	15 m 30 m 90 m	16 days	60 km	Bathymetry, vegetation, land use and land cover, change detection, circulation, geomorphology
t2.16 t2.17 t2.18 t2.19	LANDSAT-7	450–2,080 nm 10,420 nm	6VNIR 1TIR 1Pan	30 m 60 m 15 m	16 days	180 km	Wide range of application on coastal resources (e.g. determining patterns and extent of turbidity) and land use and land cover and mapping (e.g. categorizing land capabilities)
t2.20 t2.21 t2.22	LANDSAT-8	433–2,300 nm 1,030–1,250 nm	8VNIR 2TIR 1Pan	30 m 100 m 15 m	16 days	185 km	
t2.23 t2.24 t2.25 t2.26 t2.27 t2.28 t2.29 t2.30	SPOT 1-2-4-5	500–890 nm	3MS 1Pan	20 m 10 m	26 days daily	60 m	Wide range of application (e.g. land cover and change detection, water temperature, salinity, phytoplankton, hydrology, shoreline changes, erosion, bathymetry and habitat mapping)

(continued)

Table 3.2 (continued)

Satellite/sensor	Spectral range	Bands	GSD	Revisit time	Swath width	Application
WorldView-2	450–1,040 nm	8MS	2	1.1–2.7 days	16.4 km	Bathymetry, vegetation, littoral processes, coastal geomorphology, digital elevation models
		1pan	0.5			
GeoEye-1	450–920	4MS	1.65	2.1–8.3 days	15.2 km	
		1Pan	0.41			
IKONOS	450–750	4MS	4 m	1–3 days	13 km	
		1Pan	1 m			
Quick bird 2	450–900 nm	4MS	4 m	<3 days	22 km	
		1Pan	1 m			
Orbview 3	450–900 m	4MS	4 m	<3 days	8 km	
		1Pan	1 m			
Orbview 4	450–2,500 nm	200HS	8 m	<3 days	5 km	
	450–900 nm	4MS	4 m			
		1Pan	1 m			
ALIEO-1	400–2,400 nm	9MS	30 m	19 days	37 km	Bathymetry, vegetation, land use and land cover, change detection, circulation, geomorphology
		1Pan	10 m			
Hyperion EO-1	400–2,400 nm	220	30 m	16 days	8 km	Bathymetry, vegetation, littoral processes
NEMO/COIS	400–2,500 nm	210	30 m			
MERIS ENVISAT-1	290–1,040	15	300 m	<3 days	1,150 km	Ocean color, circulation
ASAR ENVISAT-1	C-band 4 pol	2	30 m	<3 days	50–100 km	Circulation, waves
AMI ERS-2(SAR)	C-band V pol	1	25 m	28 days	100 km	
RADARSAT-1(SAR)	C-band H pol	1	6–100 m	1–4	20–500 km	Oil spill, internal waves and altimetry
RADARSAT-2(SAR)	C-band HV pol	1	3–100 m		20–500 km	

spectral bands of WorldView-2 enable more accurate retrievals of water quality parameters from the reflectance values.

3.2.2 Object-Based and Pixel-Based Classifications

The literature regarding the discussion about the difference between Pixel-Based (Supervised and Unsupervised) and OBIA classification has been very active in the last years, and a large number of papers regarding the classification accuracy of this RS techniques have been published (Gutierres 2014; Teodoro and Gonçalves 2011; Weih and Riggan 2010; Gao and Mas 2008; Lillesand et al. 2008; Rahman and Saha 2008; Blaschke and Lang 2006; Hay and Castilla 2006; Hall et al. 2004; Hay et al. 2003; Lang and Blaschke 2003; Foody 2002; Baatz and Schäpe 2000).

The most popular techniques are those based on group pixels – unsupervised and supervised image classifications – to represent land cover features such as wetlands and beaches. There are different image clustering algorithms such as K-means and Iterative Self-Organizing Data Analysis Technique (ISODATA) (Lillesand et al. 2008).

The supervised classification is based on the spectral signature defined in the training set. The most usual supervised classification algorithms are Maximum Likelihood (MLC), Minimum-

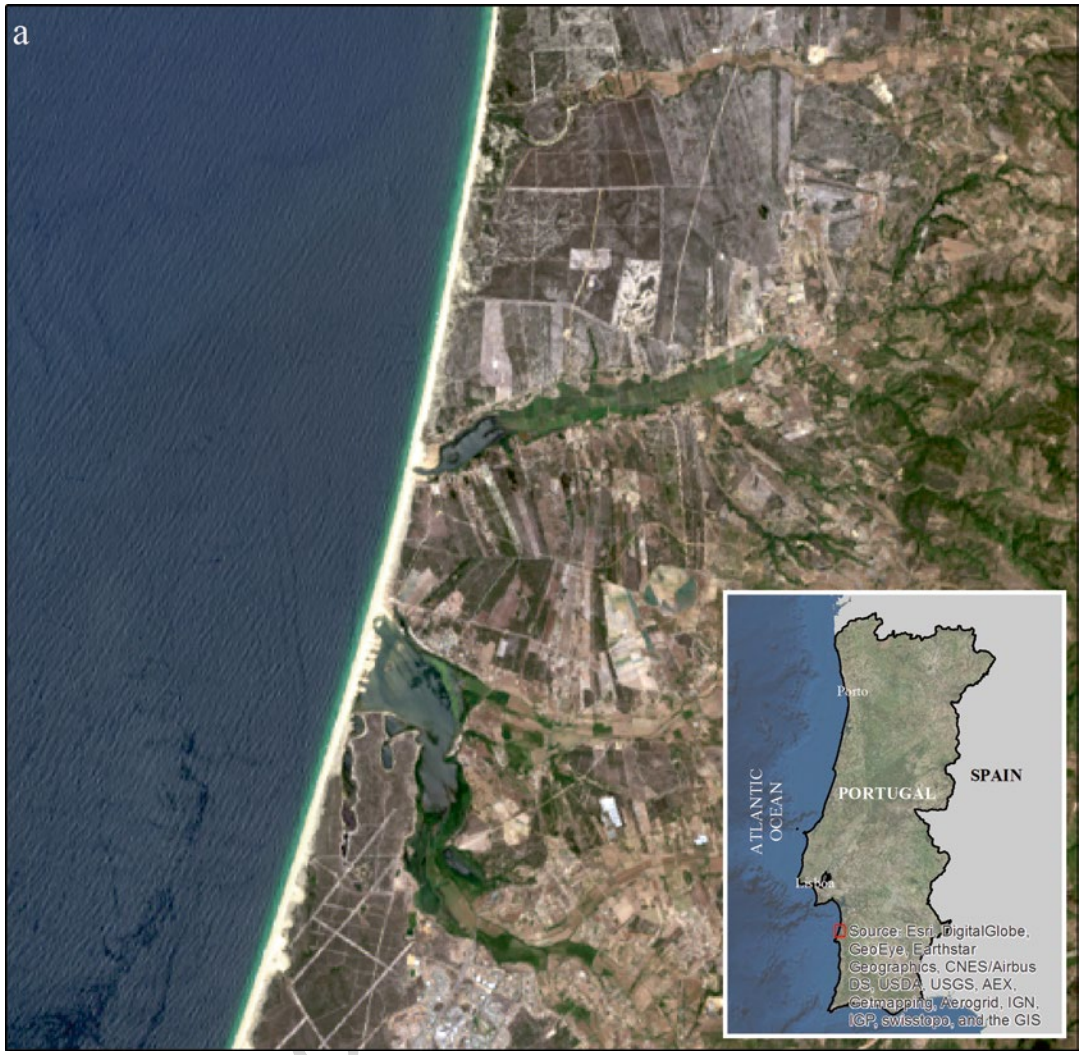

Fig. 3.1 Subset of LANDSAT-8 scenes from coastal lagoons on the Portuguese southwest coast. Image acquired in 25 May 2015 over 'Santo André' lagoon. (**a**) Natural color composite of the Operational Land Imager (*OLI*) *red* (0.64–0.67 μm), *green* (0.53–0.59 μm) and *blue* (0.45–0.51 μm). (**b**) Color infrared (vegetation) composite of the OLI near infrared (0.85–0.88 μm), *red* (0.64–0.67 μm) and *green* (0.53–0.59 μm). (**c**) Land water composite of the OLI near infrared (0.85–0.88 μm), shortwave infrared (1.57–1.65 μm) and *red* (0.64–0.67 μm). (**d**) Six hundred fifty four false color (vegetation analysis) composite of the OLI shortwave infrared (1.57–1.65 μm), near infrared (0.85–0.88 μm) and *red* (0.64–0.67 μm)

Distance-to-Means (MDM) and Parallelepiped classifiers.

According to Lillesand et al. (2008), the mixed pixels (includes more than one land cover type or feature on the ground) present a difficult problem for image classification, since their spectral characteristics are not representative of any single feature. Spectral mixture analysis and fuzzy classification are two procedures designated to deal with the classification of mixed pixels. All of these pixel-based processing methods generate square classified pixels.

Instead, the OBIA classification generates objects of different shape and scale. Hay and Castilla (2006) defines OBIA as a sub-discipline of GIScience devoted to partitioning RS imagery

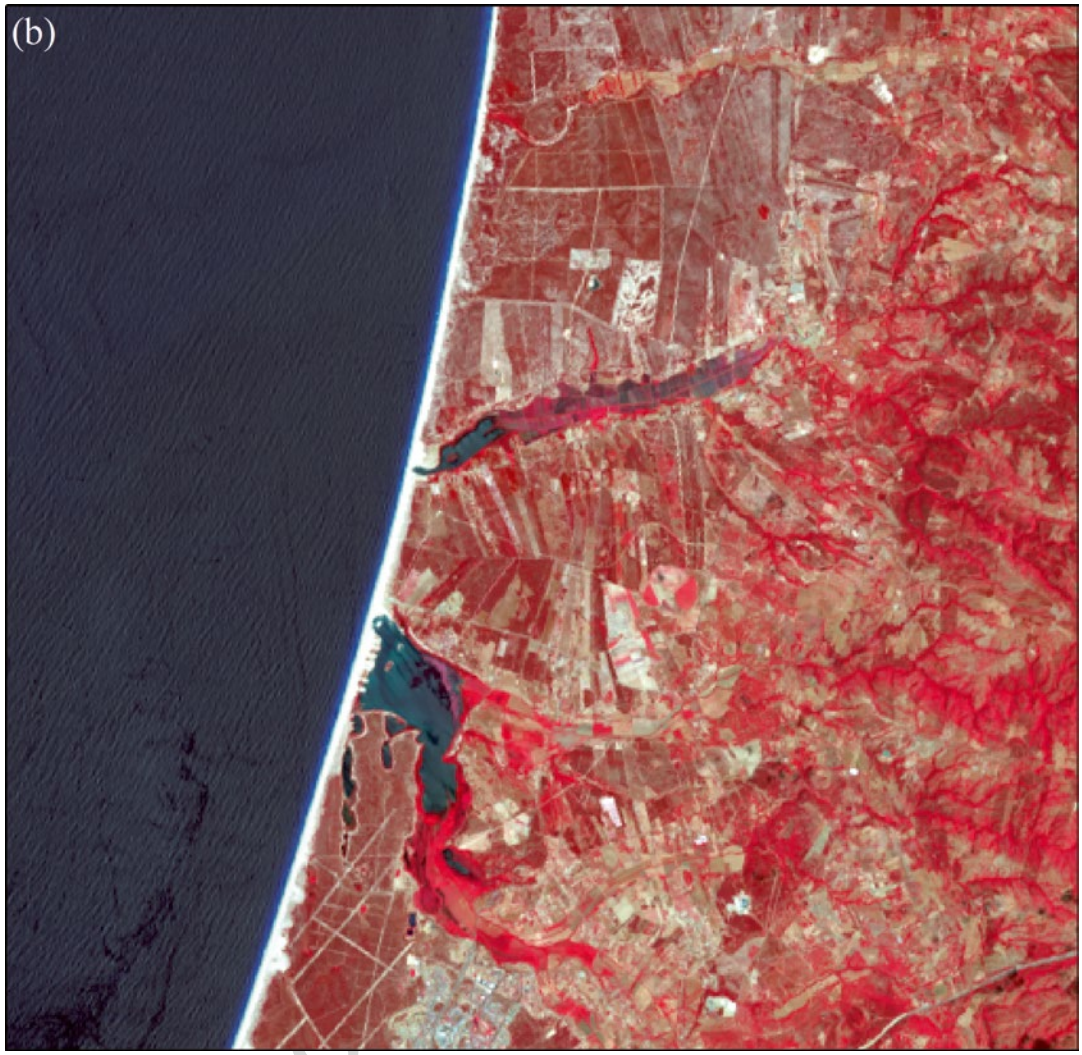

Fig. 3.1 (continued)

into meaningful image-objects, and assessing their characteristics through spatial, spectral and temporal scale. At its most fundamental level, OBIA requires image segmentation, attribution, classification and the ability to query and link individual objects (segments) in space and time. Image segmentation is commonly divided into five categories: (a) point-based, (b) edge-based, (c) region-based; (d) combined – watershed and multi-resolution (Fig. 3.3) (Schiewe 2002; Baatz and Schäpe 2000; Pal and Pal 1993).

No matter which of the methods is applied, segmentation produces homogeneous image objects by grouping pixels, and is typical used to locate objects and identify boundaries (Gutierres 2014; Teodoro and Gonçalves 2011; Hay and Castilla 2008; Lang 2008). Several marine/costal studies require the segmentation of natural spectral classes such as open water bodies (Lira 2006; McFeeters 1996; Daya-Sabar et al. 1995), wetland habitats (Gutierres 2014), river plume size (Teodoro and Gonçalves 2011; Valente and da Silva 2009; Nezlin et al. 2005; Otero and Siegel 2004), physical differences (e.g. salinity) between the estuarine outflow and the ambient water (Dzwonkowski and Yan 2005), suspended sediments (Nechad et al. 2010; Teodoro et al. 2007a, b;

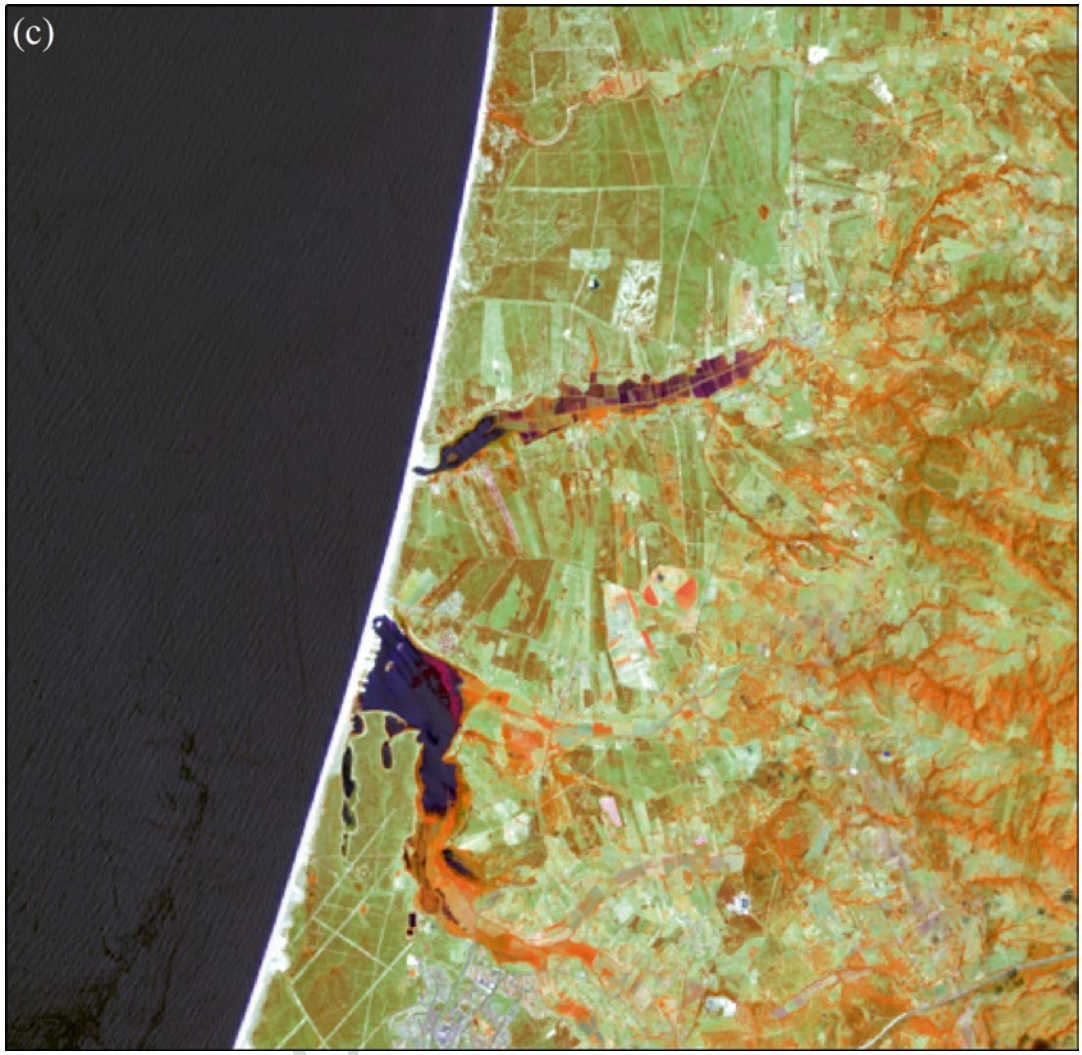

Fig. 3.1 (continued)

Lira et al. 1997) and sand spits (Teodoro and Gonçalves 2011; Bird 2008). So these objects are more meaningful than the traditional pixel-based segmentation because they can be classified based on texture, context and geometry (Teodoro and Gonçalves 2011; Rahman and Saha 2008; Baatz et al. 2001) (Fig. 3.4).

Another advantage is the OBIA allows the use of multiple bands for the multiresolution segmentation and classification (e.g. automated vegetation mapping based on WorldView-2) (Fig. 3.5) (Gutierres 2014).

Weih and Riggan (2010) compared OBIA and Pixel-Based classification, and showed that when merging a high-spatial resolution color infrared digital orthophoto with multitemporal (winter and spring) medium-spatial resolution SPOT-5 satellites images, an OBIA classification outperform both supervised and unsupervised Pixel-Based methods. Also the OBIA clearly reduced the "salt and pepper" effect presented in Pixel-Based classification, and may appear more visually attractive to the analyst.

The research developed by Gao and Mas (2008) has shown that with satellite imagery of four different spatial resolutions (SPOT-5, LANDSAT-7 ETM+ and MODIS), OBIA obtained higher accuracies than those of the

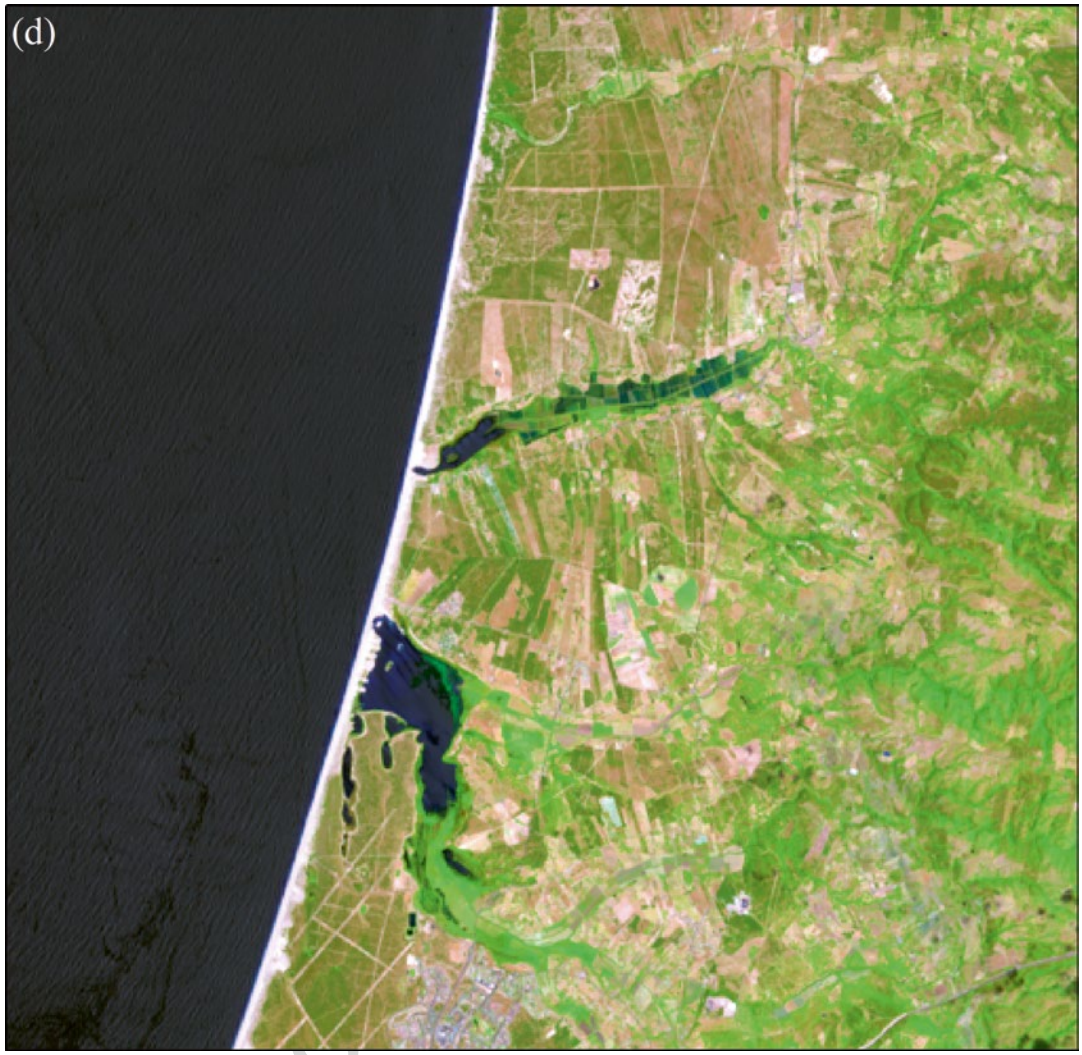

Fig. 3.1 (continued)

Pixel-Based one. Thus with the increase of the pixel size (10, 30 and 250 m), OBIA did not show more advantage over the Pixel-Based ones. The authors proved that OBIA has advantage over the Pixel-Based method but the higher accuracy only holds true for high spatial resolution images.

Gutierres (2014) applied a hybrid method (combination of Pixel-Based classification and multi-resolution segmentation) and found that the inclusion of image-objects for the Natura 2000 habitat classification lead to higher accuracy levels.

In conclusion, it was recognized that Pixel-Based image analysis reveals limitations because the following reasons:

- Image pixels are not true geographical objects and the pixel topology is limited;
- Pixel-Based image analysis largely neglects the spatial photo-interpretive elements such as texture, context and shape;
- The increased variability implicit within high spatial resolution imagery confuses traditional Pixel-Based classifiers accuracy (Hay and Castilla 2006).

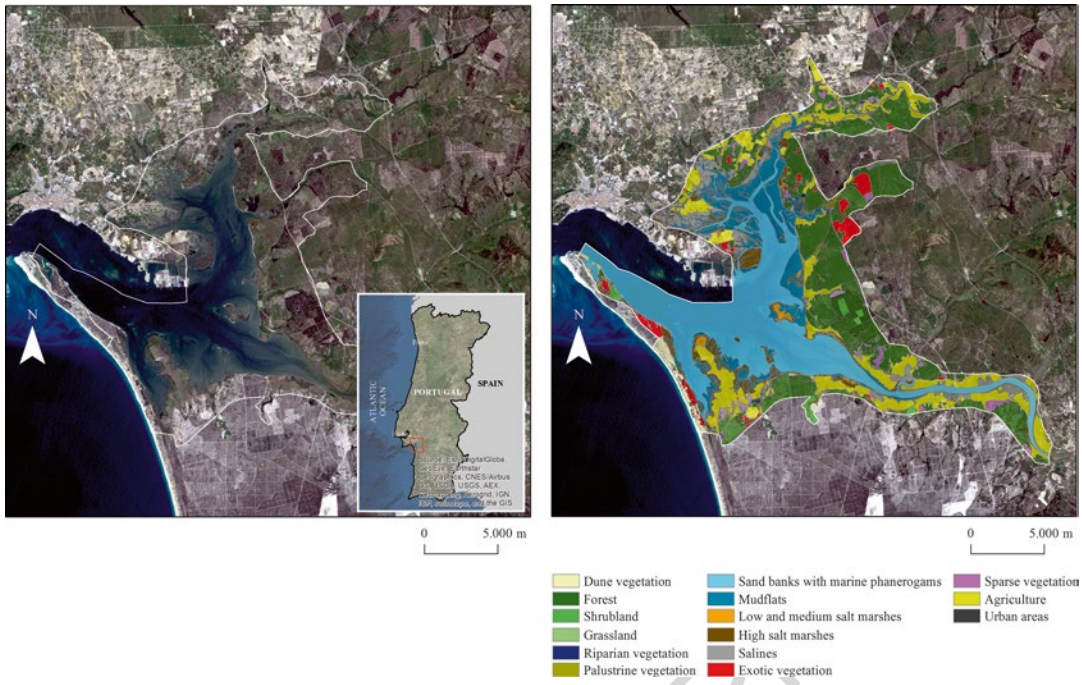

Fig. 3.2 Sado Estuary land cover classification based on LANDSAT-7 ETM+. Image acquired in 25 April 2010 over Site of Community Importance (*SCI*) of the Sado Estuary

Fig. 3.3 Multi-resolution segmentation of WorldView-2 image data: water bodies and wetland vegetation are of similar spectral values. Image acquired in 11 June 2011 over the fluvial-lagoon system of 'Santo André-Monte Velho'

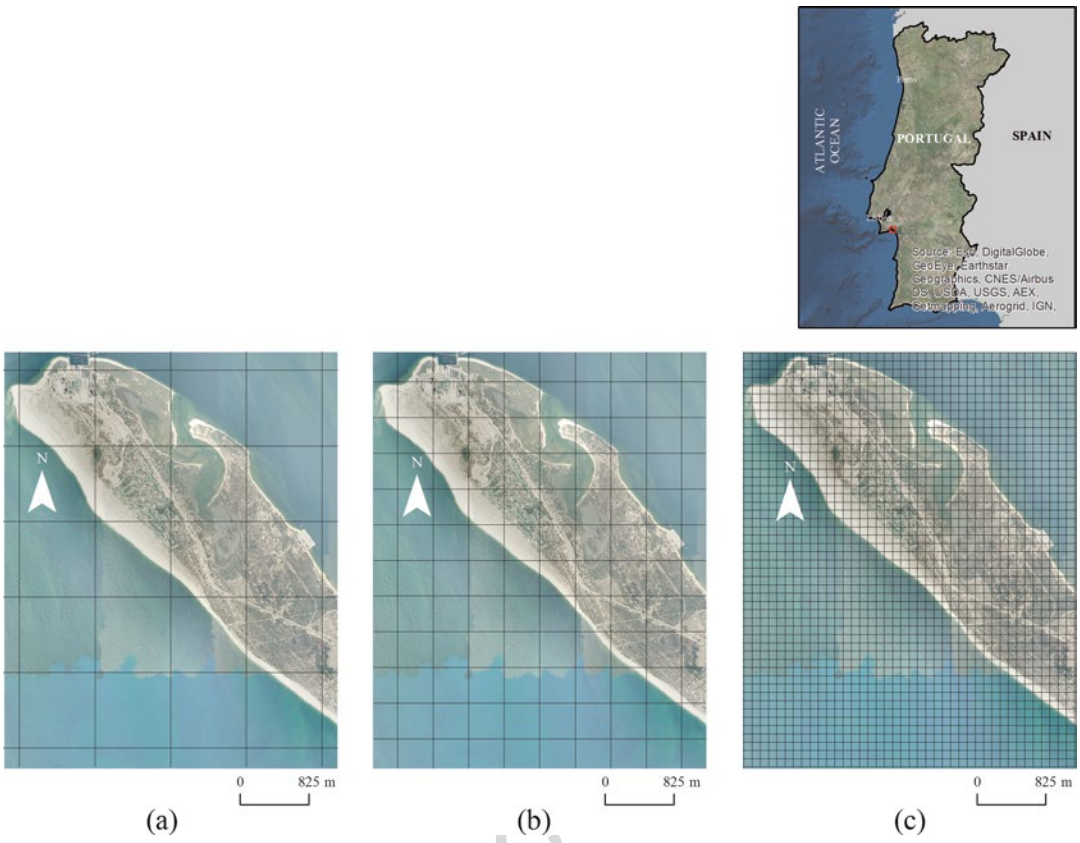

Fig. 3.4 Spatial resolution of the imagery: Low | Medium | High. (**a**, **b**) Low-medium spatial resolution – pixels and objects are similar in scale. Traditional pixel-based and object-based image classification techniques perform well. (**c**) High spatial resolution – objects are made up of several pixels. In this case, object-based image analysis is superior to traditional pixel based classification. Orthophoto four bands (R, G, B and NIR) of the Tróia Spit acquired in 22 April 2007 (From General Directorate for the Territory (DGT), 2011, with permission)

Instead, OBIA is centered on homogeneous objects produced by image segmentation and more elements can be use in classification. Thus object characteristics such as mean and standard deviation values of spectral bands, ratio, etc., can be calculated; besides there are shape and texture properties of the image objects available which can be used to differentiate marine and coastal features with higher accuracy than those produced by the Pixel-Based method.

3.2.3 What Needs to Be Improved

Recent advances in sensor design are making RS systems more attractive for assessment of marine and coastal ecosystems, such as open sea, wetlands, estuaries, and coastal lagoons. Generally, these ecosystems presents high spatial complexity and temporal variability, their assessment can be improved from new satellite imagery and aircraft, to allow getting better systematic, spatial, spectral, and temporal resolutions.

Currently we consider that the assessment of marine and coastal ecosystems can be improved considering the launch in June 2015 of the sentinel-2 satellite within Copernicus project of the European Space Agency (ESA). This will be an Earth Observation (EO) operational mission providing continuity to LANDSAT data. It has a global coverage of the Earth's land surface every 10 days with one satellite and 5 days with two

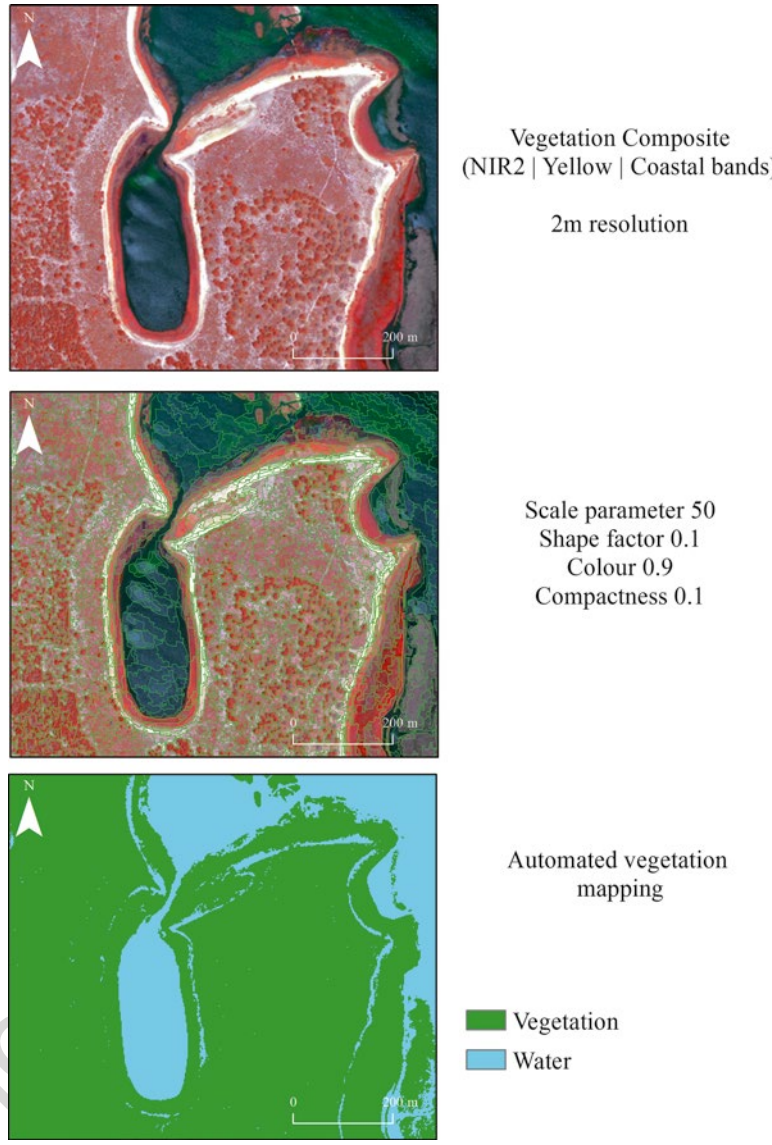

Fig. 3.5 Water bodies and vegetation units classification based on OBIA rule sets for the automatic analysis of remote sensing data. Image acquired in 11 June 2011 over the fluvial-lagoon system of 'Santo André-Monte Velho'

satellites that will able to monitor continuously the water quality and flood dynamics.

Further studies with new sensors must be developed for monitoring the marine and coastal areas. The usage of Sentinel-2 sensor, time series of very high resolution imagery (e.g. WorldView-2), hyperspectral sensors, airborne Light Detection and Ranging (LiDAR) systems, Thermal infrared scanners, microwave radiometers, Radar images, scatter meters, altimeters, Unmanned Aerial Vehicle (UAV) and new data analysis techniques can provide the way forward for future prospects, such as, raise the accuracy of change detection in costal ecosystem health (e.g. wetland biomass change); detailed mapping of sea surface temperatures, salinity and soil moisture; deep analysis of sea surface winds, elevation, currents, wave fields and oil slicks; improvement of shoreline position analysis and beach erosion studies; and a better performance high-resolution three-dimensional measurements of biological and physical ocean features.

Also accurate field data collection approach using ships, buoys, and field instruments with a

valid sampling scheme must be improved to calibrate and/or validate the remotely sensed information.

3.3 Management of Marine and Coastal Ecosystems through RS Applications

In this section were provided examples of using RS technologies in applications relevant to management of marine and costal ecosystems needs. Were presented and discussed six cases related to marine/coastal management and monitoring efforts in the Portuguese coast.

3.3.1 Landscape Scale Analysis of Coastal Wetlands Health and Land Cover Changes

Wetlands are ecologically sensitive and dynamics ecosystems susceptible to climate and LULC changes, and support high levels of biodiversity. Over the last centuries its conservation status has been neglected, and in several cases have been forced to drainage and transformations. The first international convention on Wetlands of International Importance (formally, the Ramsar Convention was signed in 1971) aimed the conservation and sustainable utilization of wetlands, recognizing the fundamental ecological functions of wetlands (such as water regulation, filtering and purification) and their economic, cultural, scientific, and recreational value. The United Nations Millennium Ecosystem Assessment recognizes the global economic value of wetlands (at up 15 trillion USD in 1997) (Bustamante et al. 2013). Such ecosystems include areas with biologically valuable vegetation, such as, peat bogs, marshes and tidal flats. An increasing number of wetlands have some kind of legal protection, such as National Reserves, Site of Community Importance (SCI), Special Protected Zones (ZPE) or Important Bird Areas (IBA)), and several coastal wetlands are constantly monitored and managed (Correia et al. 2012; Freitas et al. 2007).

RS provides useful information and tools to identify long-term trends and short-term variations, such as impact of rising sea levels and LULC changes on wetlands. For instance, Bustamante et al. (2013) mentioned that EO satellites can be used to delineate flooded areas, and can supply complementary information on wetland location, limits and extent. They can also be used to monitor changes in water quality (cyanobacterial blooms, trophic status, inputs of terrestrial Carbon), to map habitat types, vegetation communities, to identify long-terms trends and subtle changes of biomass, or ecosystem services (Mücher et al. 2010; Kennedy et al. 2009).

Thus, RS can provide methods to monitor specific biophysical and biochemical indicators of ecosystem functioning (e.g. Leaf Area Index (LAI), Normalized Difference Vegetation Index (NDVI), chlorophyll content, fractional cover, phenology, vegetation height (Mücher 2009; Kerr and Ostrovsky 2003). Many of these parameters are currently mainly applied at large scales (global, continental), see e.g. the Core Services on Bio-Geophysical Parameters of the EC-funded Geoland project (GMES for Europe), which aim at facilitating policy-supporting applications in the fields of climate change (carbon fluxes), food security (crop monitoring), and global land cover change. The relation of such parameters with the more traditional habitat quality approach at the scale of the habitat patch is still to be investigated.

Changes in wetland vegetative cover, which can be expressed as NDVI, manifest as changes of species composition and productivity, are generally the result of dynamics processes and anthropic induced perturbation. Thus, the NDVI can be related to plant biomass or stress, since the NIR reflectance depends on the abundance of plant tissue and the red reflectance indicates the surface condition of the plant (Klemas 2011). Frequently, these major transitions in wetland systems are preceded by gradual degradations of native habitats. These modifications of existent habitats, while not always altering areal extent, can modify the functional health of coastal wetlands. Thus RS would be more useful for wetlands research if it could include

some assessment of the functional health of the existing vegetation in addition to any changes in areal extent. The use of remotely sensed data, however, limits the number of possible indicators that can be used to monitor the health conditions of the wetlands. Fortunately, RS techniques have been successful in mapping one of the most practical indicators of wetland conditions over large areas – vegetative abundance, i.e., biomass density (Kennedy et al. 2009).

In this context, Gutierres (2014) make an attempt to elaborate RS indicators of coastal wetlands integrity and trends in Santo André Lagoon. According to Correia et al. (2012), Santo André is the largest lagoon (500 ha) on the Alentejo coastline, belongs to the Santo André and Sancha Natural Reserve, and represents an enclosed brackish water coastal lagoon with temporary connections to the sea by a man-made channel. The existence of fresh and brackish waters gives rise to a diverse set of aquatic ecosystems and riparian areas that include small marsh areas, willow plantations, rush and reed beds, bogs, heathland and wetland pastures. The exchange and mixture of saltwater and freshwater is irregular and the lagoon may show daily and seasonal fluctuations, but also long-term variation. Different benthic communities may be present along the annual cycle according to the magnitude of episodic freshwater and sea water inputs.

Therefore the goal of this investigation was to use remotely sensed data in a Geographical Information System (GIS) framework in order to integrate and evaluate Land Use and Land Cover (LULC) changes and wetland conditions indicators which are important for determining and managing wetland health. The specific objectives were:

- To determine whether environmentally stressed wetland areas can be identified through the analysis of a normalized time-series (LANDSAT TM of 1989, 2000, 2007 and 2010), namely by the combination of the NDVI (biomass) maps with ancillary LULC layers (Corine Land Cover (CLC) Changes 1990–2000 and 2000–2006).
- To develop long-term monitoring techniques for evaluation of trends in wetland conditions and thus improve the management of wetland ecosystem.
- To determine if LULC and water quality data in the GIS database can be used to relate water quality changes to changes in surrounding land use and nonpoint source pollution loadings.

The biomass abundance maps of Santo André lagoon, obtained through NDVI reclassified into five biomass density classes, revealed useful to identify the most fragile areas, where management actions for conservation should focus on the future (Fig. 3.6).

Thus, were found that RS techniques can be used effectively in a GIS framework with ancillary data to provide valuable information of the management of Santo André lagoon. The strength of RS is its ability to deliver quantitative measures of such parameters in a standardized manner with full coverage over larger wetland areas, whereas field surveys can only deliver this through point sample measurements and subsequent interpolation. The provision of such data by RS may open new ways of looking at quality of coastal wetlands. This becomes especially relevant as higher resolution, lower cost satellite data become available and RS techniques for analyzing spatial data set improve.

3.3.2 Integration RS in Natura 2000 Habitat Monitoring

Monitoring and reporting on the conservation status at local level, Site of Community Importance (SCI), gained increasing importance in the European Union with the implementation of the Habitat Directive in 1992 (Council Directive 92/43/EEC of 21 May 1992 on the conservation of natural habitats and of wild fauna and flora) (Gutierres et al. 2013; Vanden Borre et al. 2011). According to Article 17 of the Directive, reporting the habitat conservation status requires detailed knowledge of

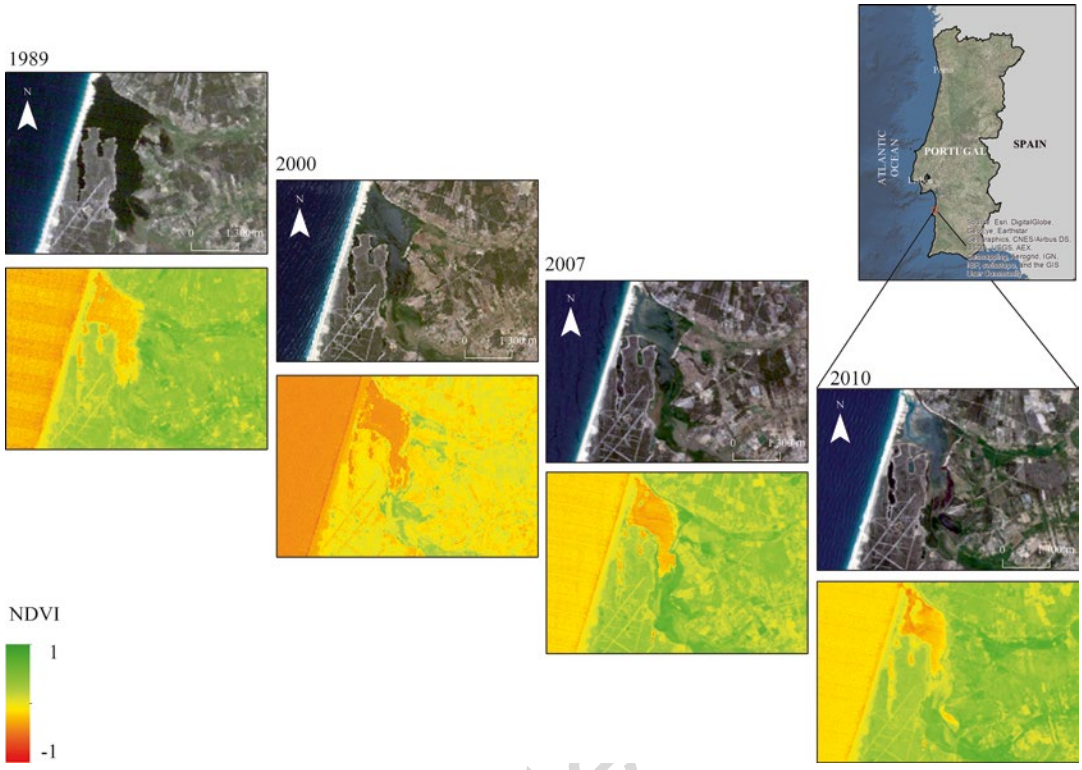

Fig. 3.6 NDVI (Biomass) change analysis based on LANDSAT-7 ETM+ (1989–2010). Images acquired in 14 March 1989, 24 June 2000, 22 July 2007 and 25 April 2010 over 'Santo André' coastal lagoon

many aspects of Natura 2000 habitats at different spatial scales (Evans 2006).

According Vanden Borre et al. (2011), RS is seen as an important tool to obtain and analyze synoptic data on Natura 2000 habitats, but currently reflects some limitations for monitoring and reporting purposes.

In fact, the application of RS tools for habitat mapping and monitoring offers multiple advantages over traditional field mapping, like faster map production, insight into remote and inaccessible terrain such as coastal wetlands, and improved repeatability of the habitat mapping process (Blaschke et al. 2008; Lengyel et al. 2008; Groom et al. 2006; Aplin 2005; Bock et al. 2005a, b; Keramitsoglou et al. 2005; Nagendra 2001; Buiten and Clevers 1990).

In the application field of Natura 2000 habitat mapping and monitoring, the RS analysis is restricted to pilot studies (e.g. Mücher 2009; Diaz Varela et al. 2008; Förster et al. 2008; Bock et al. 2005a; Frick et al. 2005). According Bock et al. (2005b), in the past RS techniques fell short in mapping very detailed and particular biotopes like Natura 2000 coastal habitats, but RS capabilities is evolving rapidly, and new methodologies are opening up opportunities for innovative applications of RS data in habitat monitoring (Gross et al. 2009; Aplin 2005; Turner et al. 2003).

Gutierres (2014) produced detailed Natura 2000 habitat maps contained in the fluvial-lagoon system of Santo André-Monte Velho (Fig. 3.7). This lagoon system is included in the 'Lagoas de Santo André and Sancha Natural Reserve', which occupies a 15 km-wide coastal sector inland from the shoreline, on the Alentejo coastline in the municipalities of Sines and Santiago do Cacém. The Natural Reserve includes the Lagoa de Santo André (500 ha) and the Lagoa da Sancha (15 ha), a dune system (mobile and stabilized dunes), shrublands and

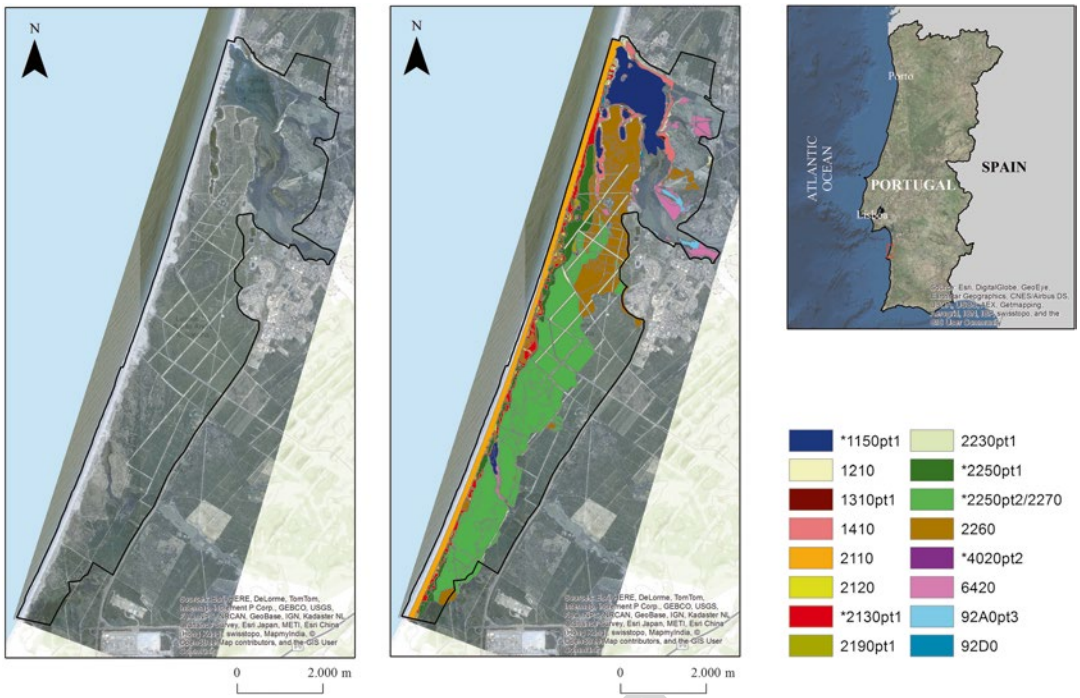

Fig. 3.7 Mapping the local variability of Natura 2000 habitats with WorldView-2 image data (Image acquired in 11 June 2011 over the fluvial-lagoon system of 'Santo André-Monte Velho')

Pines formations and a small ponds system with peat bogs and humid shrublands (designated as "Poços"). Its protected status recognizes the high ecological value of these two wetlands and their surrounding areas which also include the ridge of dunes that separates them from the ocean and the adjacent seashore.

The study was carried out with Very High Spatial Resolution Satellite (VHSR) Imagery – GeoEye-1 and WorldView-2 covering Santo André-Monte Velho lagoon system. Table 3.3 lists the detailed specifications of GeoEye-1 and WorldView-2 satellite images.

In addition to the standard panchromatic and multispectral blue, green, red (visible) and Near InfraRed (NIR1) bands the WorldView-2 sensor has:

(a) A shorter wavelength blue band, Coastal Blue, planned for bathymetric studies, can be used for water color analyses and substantially influenced by atmospheric scattering;
(b) A Yellow band can be used for the assessment of the Yellowness of vegetation both on land and water;
(c) A Red Edge band, centered at the onset of the high reflectance portion of vegetation response to potentially significant in the measurement of plant health;
(d) A longer wavelength Near InfraRed band (NIR2), partially overlapping the NIR1 was sensitive to atmospheric water vapor absorption.

Two different approaches were used in order to mapping the Natura 2000 habitats:

1. Based on GeoEye-1 image was developed a spectral separability study and application of the combined approach (spectral and spatial domains), based on pixel-based classification and OBIA (hybrid method).

Table 3.3 High-resolution satellite parameters and spectral bands (Satellite Imaging Corporation 2015)

Parameter	Spectral band	*GeoEye-1*	*WorldView-2*
Date launched		September 2008	October 2009
Spatial resolution (m)	Panchromatic	0.41	0.5
	Multispectral	1.65	2
Spectral range (nm)	Panchromatic	450–800	450–800
	Coastal blue	n/a	400–450
	Blue	450–510	450–510
	Green	510–580	510–580
	Yellow	n/a	585–625
	Red	655–690	630–690
	Red edge	n/a	705–745
	NIR	780–920	770–1,040
	NIR1		770–895
	NIR2		860–1,040
Swath width (Km)		15.2	16.4
Off nadir pointing		±30°	±45°
Revisit time (days)		2.1–8.3	1.1–2.7
Orbital altitude (Km)		681	770
Image acquisition dates		15th June 2011 at 11:35 AM	11th June 2011 at 11:55 AM

2. The second methodological approach was based on producing habitat maps through Segmentation-based Supervised Classification of the WorldView-2 image data, instead of the pixel-based classification approach.

The detailed methodologies of the hybrid approach and supervised OBIA procedures are presented and compared in Gutierres (2014). The accuracy of the classification maps was estimated using a set of test fields randomly selected on the ground truth map.

This analysis showed that the eight-band sensor is extremely useful to better discriminate different spectral sub-signatures corresponding to the same habitat category. This means that the major capability of the new sensor resides in the capacity of investigating the ground diversity underlying the apparent homogeneity of conventional habitat map. From the Segmentation-based Supervised Classification approach, it was possible to detect changes in the bathymetry for the Sea Water classes by using the Coastal Blue band; moreover, the lowest wavelength band appears to be significant for the recognition of mixed patterns of water and terrain. The Yellow band appears significant to elicit terrain composition, as characterized by a certain degree of yellowness. The Red Edge and the NIR2 bands were useful for a better discrimination of ground sites characterized by a mixing of water and vegetation. The increase in thematic accuracy was 15 %, passing from the traditional four band provided by GeoEye to the new eight-band WorldView-2 sensor. In fact, the overall separability of vegetation classes and water bodies was improved with WorldView-2 and significantly after the training data depuration process of coastal habitats. The results obtained proved that the VHSR integration can contribute to the area (location and size) monitoring and also to assess the structure and function (particularly regarding structural features) of the Natura 2000 coastal habitats at local scale.

Concluding, the production of coastal habitat distribution maps, at various scale levels, constitutes a promising new area for the development of RS applications, as Vanden Borre et al. (2011) indicated. The emergence of hyperspatial and hyperspectral sensors will enhance the analysis of related habitat types at very fine scales (see Haest et al. 2010; Lechner et al. 2009; Mehner

et al. 2004). The researchers need such RS-based habitat mapping for estimating range and area of coastal habitats, but also to achieve a better definition and constant updating of the sampling frame for Natura 2000 habitats survey. Indeed, RS technologies represent an important opportunity for harmonizing Natura 2000 habitat mapping throughout Europe.

3.3.3 Quantification of the Total Suspended Matter (TSM) Concentration in Case-2 Waters

Major factors affecting water quality in water bodies across the landscape are suspended sediments, algae, chemicals, DOM, thermal releases, aquatic vascular plants, pathogens, and oils. Satellite sensors with different spectral, spatial, and temporal resolutions have been used to evaluate chemical pollutants, suspended solids, and chlorophyll abundance (Godin et al. 1993).

The dominant optically active constituent in the open sea (case-1 waters) is the chlorophyll, whereas in the coastal waters (case-2 waters), sediments and DOM often dominate the spectral signal of chlorophyll (Myint and Walker 2002). The study of suspended matter has an ecological importance, because the suspended matter is the main carrier of various inorganic and organic substances and becomes the main substrata for biochemical processes (Doeffer et al. 1989). The TSM concentration affects ocean/coastal productivity, water quality, navigation, and coastal defense. The TSM concentration and distribution in the coastal zone varies with several hydrodynamic factors, such as tidal condition, currents direction and velocity, river discharges, and wind stress (Teodoro et al. 2007b). The discrimination of TSM from water reflectance is based on the relationship between the scattering and absorption properties of water and its constituents. In the visible and NIR region, most of the scattering is caused by suspended sediments, and the absorption is controlled by chlorophyll-a and colored DOM. These absorptive in-water components decrease the reflectance in a substantial way. However, these absorptive effects occur generally for wavelengths less than 500 nm (Myint and Walker 2002). The visible and NIR regions are the most adequate to estimate the TSM concentration.

Several works have demonstrated that remotely sensed data can be used to retrieve TSM concentration from turbid coastal waters (e.g. Nechad et al. 2010; Ouillon et al. 2008; Miller and Mckee 2004). Moreover, various studies have been carried out combining in situ measurements and satellite data in order to relate spectral properties of seawater and TSM concentration (e.g. Chen et al. 2014; Teodoro et al. 2008). Many TSM models based on empirical methods have been used in operational satellite RS systems. These models were developed on the basis of statistical relationships between TSM concentrations and single-bands or multi-bands reflectance. For instance, Doxaran et al. (2002), Islam et al. (2001), Forget and Ouillon (1998), and Ritchie et al. (1974) established empirical relationships between reflectance of visible and NIR bands of satellite data and TSM concentration. Aguirre-Gomez (2000) investigates the linear relationship between in situ measurements of TSM concentration, collected by ship, and remotely sensed data provided by AVHRR. Although empirical models may be effectively applied to satellite images concurrent with the calibration dataset, their accuracy may be reduced outside the conditions of the calibration dataset because of the empirical basis (Nechad et al. 2010). Therefore, semi-analytical models which combine physical methods with statistical methods were proposed for several authors in order to retrieve the TSM concentration (e.g. Chen et al. 2014, 2013; Ouillon et al. 2008).

Teodoro et al. (2007b) retrieve the TSM concentration from multispectral satellite data (LANDSAT TM, SPOT HRVIR and ASTER) by multiple regression and Artificial Neural Networks (ANN) for a very dynamic area of coastal zone: the breaking zone. In this work, a part of the northwest coast of Portugal, around Aveiro city, was chosen as a study site. This area is limited to the North by the Douro River mouth and to the South by Mira Lagoon (Fig. 3.8).

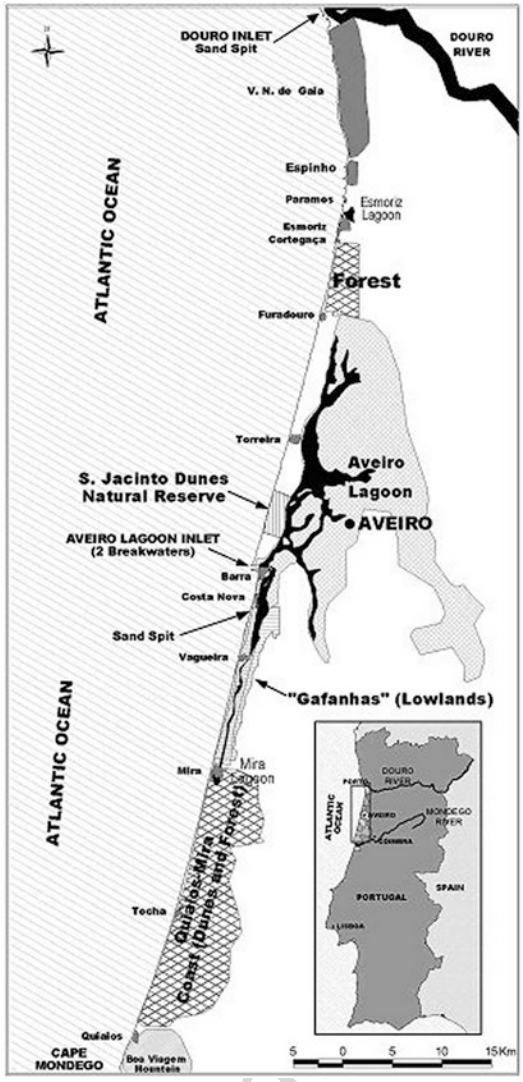

Fig. 3.8 Study area located between the River Douro mouth and Mira Lagoon (Teodoro and Veloso-Gomes 2007)

The total extension of this area is about 80 km with an orientation NNE-SSE. The littoral drift current act principally in the North-south direction. The wave climate has medium significance with wave heights from 2 to 3 m and periods ranging from 8 to 12 s. Tides are of semidiurnal type, reaching a range of 2–4 m for Spring tides. Meteorological tides are not significant.

There is a general consensus that, in cases when waves are breaking, the sediment transport tends to be directed offshore due to the seaward-directed undertow generated by wave breaking and radiation-stress decay (Aagaard et al. 2002). This fact presents a huge challenge for the researches. Over the last decades, the phenomenon of coastal erosion had been increasing progressively almost in all world coastal areas. The main causes of this serious environmental problem have been identified as a coastal response to the weakening of the river basin sediment sources and river-sediment transport, the mean sea-level rise, the human occupation of the waterfront, and dune destruction. Therefore, the determination of the TSM concentration around the breaking zone would provide meaningful information to estimate the sedimentary balance in this area.

Two different approaches were followed in order to relate the TSM concentration with the spectral response of the breaking zone water: field surveys and satellite images. In the field work different techniques were tested: maritime platforms, aerial platforms, simulations on the beach, and water samples collection in the breaking zone. It was very difficult get water samples and simultaneous radiometric measurements in the breaking zone. Therefore an evaluation of the range of TSM values, typically found in this area, need to be obtained through simulations on different beaches of the study area (Teodoro et al. 2007a, 2008; Teodoro and Veloso-Gomes 2007). In these simulations the bubbles and turbulence presented in the breaking zone were considered. A FieldSpec FR spectroradiometer was used to determine the seawater reflectance. Figure 3.9 shows the reflectance spectra (R(λ)) obtained for a range of TSM concentration with values between 14 and 449 mg/l. After, the seawater reflectance measured by the spectroradiometer was converted for the seawater reflectance recorded from ASTER, SPOT HRVIR, and LANDSAT TM in the visible and NIR bands. All satellite-image bands from visible and NIR were first calibrated for radiance values and, subsequently, for reflectance values. The atmospheric-correction procedure was based on an improved DOS technique (Chavez 1988). All satellite images were geometrically corrected using the ground-control points (GCPs) provided in the image header and further adjusted with GCPs

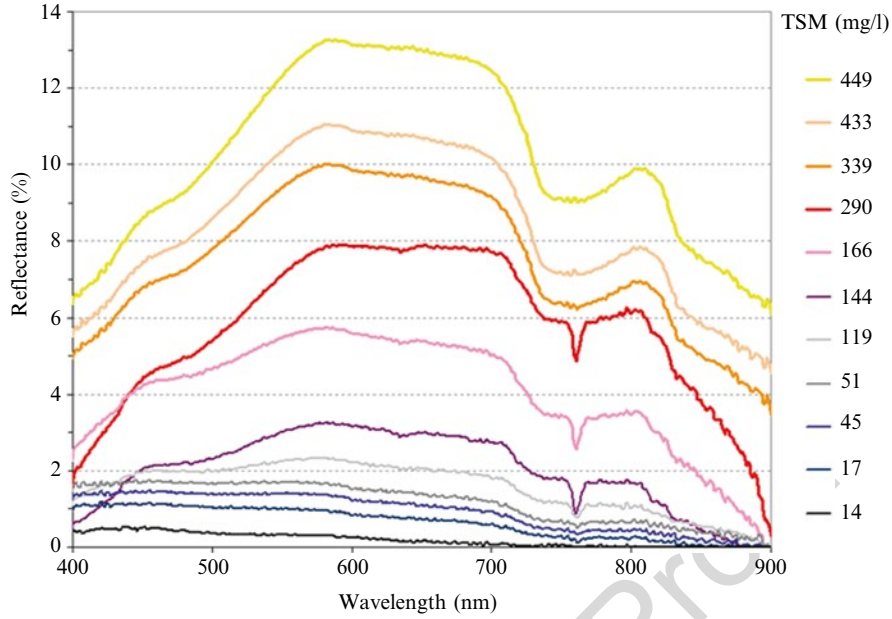

Fig. 3.9 Relationship between TSM concentration and seawater reflectance based on simulations on different beaches of the study area (Teodoro et al. 2007b)

collected in the field. The Root Mean Square (RMS) error was, for all the images, less than 1 pixel.

Three different approaches were considered in order to quantify the TSM concentration through seawater reflectance. First, single band models were proposed, and equations of linear, polynomial, logarithmic, power, and exponential models were applied for all equivalent satellite-image bands. The linear and polynomial models presented higher determination coefficient ($R^2 > 0.96$) than logarithmic, power, and exponential models ($0.63 < R^2 < 0.94$). However, the same linear models presented a Mean Absolute Error (MAE) values ranging from 20.68 to 29.28 mg/l.

After, several multiple regressions were established for the three sensors tested. The values of the dependent (TSM concentration) variable and the independent (visible and NIR reflectance, in percent) variables were used to estimate the model coefficients. The combination of the green and red bands presented high correlation coefficient values for all sensors, so this combination was discarded. The RMS error was too high, around the same TSM concentration values expected for the breaking zone (between 20 and 30 mg/l). Considering the previous results and the apparent non nonlinearity verified between the reflectance and TSM concentration, an ANN were implemented. Gan et al. (2004) have already used artificial neural networks (ANNs) to retrieve the seawater optically active parameters from multispectral and hyperspectral data. The training set of this paper consists of 11 values of reflectance of the visible and NIR channels for each sensor (inputs) and their corresponding TSM concentration values (output), already considered for the two previous methodologies. An ANN is a parallel-distributed processor that resembles the human brain by acquiring knowledge through a learning process and, then, stores the knowledge in the connection strength between computational units called neurons, and comprises several layers: an input layer; an output layer; and one or more hidden layers between them. The weights of the ANN based on the back-propagation algorithm and the leave-one-out method of error estimation. More information could be founded in Haykin (1999). Three ANN

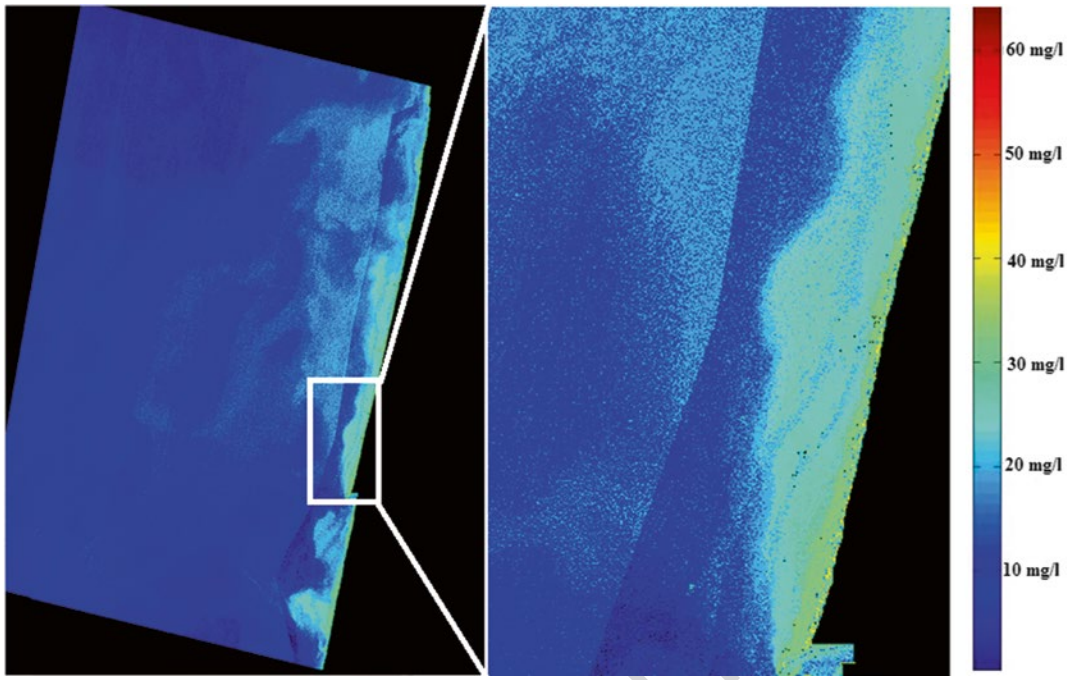

Fig. 3.10 TSM concentration estimated by the ANN implemented, considered the SPOT HRVIR image

were implemented (one for each sensor). The training set of this paper consists of 11 values of reflectance of the visible and NIR channels for each sensor (inputs) and their corresponding TSM concentration values (output). The hidden layer contains ten neurons. The algorithm stops when the RMS error is not greater than 2E-03 mg/l (an acceptable error). The final RMS errors were 1.5E-03, 4.2E-04, and 2.0E-03, for ASTER, SPOT HRVIR, and LANDSAT TM. The best results were found for ASTER and SPOT HRVIR images. In the Fig. 3.10 is presented the TSM concentration values estimated for the SPOT HRVIR image. The results are very satisfactory, as can be showed, with the discrimination between cases 1 and 2 waters and the identification of rip currents.

Concluding, the analysis of the RMS errors, achieved by both linear and nonlinear models, supports the hypothesis that the relationship between seawater reflectance and TSM concentration is clearly nonlinear. The ANNs have been shown to be useful in estimating the TSM concentration from the reflectance of visible and NIR bands from ASTER, SPOT HRVIR, and LANDSAT TM sensors, with better results for ASTER and SPOT HRVIR sensors. The nonlinearity verified between the reflectance and TSM concentration could also be related to the accuracy of the satellite-derived water leaving reflectance (atmospheric correction and calibration procedure) and also from the natural variability of water leaving reflectance from factors not directly related to TSM, such as DOM absorption or phytoplankton absorption. The accuracy of this work can be improved by enlarging the data set, synchronizing the simulations on the beach and satellite images.

3.3.4 Identification, Characterization and Analysis of River Plumes

River discharge into the coastal ocean represents a major link between terrestrial and marine systems. River plumes are an important phenomenon in coastal regions. In areas with high rates of river discharge, plumes clearly influence coastal dynamics. River plumes are a mixture of fresh

water and river sediment load, with some dilution caused by currents. The river plumes are distinguished from surround marine waters by their high concentration of total TSM which changes the color of the ocean surface. Since the TSM concentration can be associated with nutrients, pollutants and other materials, it is of crucial importance to remotely survey their dispersal in order to assess the environmental quality of the regions surrounding river mouths.

Satellite RS can provide frequent, large scale, near-surface views of the coastal ecosystem. High quality ocean color products over global open oceans are currently being produced for researchers and scientists to study and understand ocean physical, optical, and biological changes and their effects on the climate processes. However, due to physical, bio-optical, and environmental complexities of the coastal turbid waters, satellite-derived ocean color data from standard products are often biased in coastal ocean regions.

The most commonly used satellite data for river plume observations/quantification included data from AVHRR (e.g. Otero et al. 2009), SeaWiFS (e.g. Son et al. 2012; Mertes and Warrick 2001), MODIS (Fernández-Nóvoa et al. 2015; Mendes et al. 2014; Ondrusek et al. 2012; Shi and Wang 2009; Warrick et al. 2007), MERIS (Teodoro et al. 2009a) or combining data from different sensors (e.g. Jiang et al. 2009; Hendiarti et al. 2004; Warrick et al. 2004; Hu et al. 2003).

Some work has also been done using satellite sensors with higher spatial resolutions such as LANDSAT TM and ETM plus images (e.g. Guneroglu et al. 2013; Rudorff et al. 2011; Hellweger et al. 2004; Lira et al. 1997) or SPOT data (e.g. Doxaran et al. 2002; Ouillon et al. 1997). Although the increased spatial resolution provides vastly greater structural detail within the plume signatures, the low temporal resolution (approximately 2 weeks), makes image availability after a storm event a major limitation.

The Douro river is one of the longest rivers in the Iberian Peninsula and represents the most important freshwater input into the Atlantic Ocean in the north western Portuguese coast. The Douro river is a granitic drowned valley river, draining to the N-W shore of Portugal, and its basin is the largest hydrographical basin in the Iberian Peninsula. This estuary is located on the Western Portuguese coast and is subject to North Atlantic meteorological and hydrodynamic conditions. The narrow Douro estuary is limited 21.6 km upstream by the Crestuma dam.

Several studies address coastal upwelling and the dynamics of the Western Iberian Buoyant Plume under several scenarios (e.g. Otero et al. 2008, 2009). Mendes et al. (2014) develop an ad-hoc methodology to observe and characterize the Douro plume and its spatial and temporal variability by using MODIS long-term ocean-color satellite data (2003–2011) and concurrent in situ wind, tidal and river discharge data. However, little attention has been given to the influence of the Douro Estuary (Fig. 3.11) input into the coastal adjacent areas. A preliminary study on the modeling of the Douro River Plume (DRP), Douro River, Porto, Portugal, size obtained through image segmentation of MERIS data has been performed based on 21 MERIS scenes covering approximately 2 years (Teodoro et al. 2009a). More recently, a similar study of the river plume size with a larger dataset of more recent images (the hydrological year starting at October 2008) was also performed (Teodoro and Almeida 2011; Teodoro and Gonçalves 2011). Gonçalves et al. (2012) presents a work where a fully automatic method for the identification of the Douro river plume is proposed, as well as a more complete characterization of the river plume, through several attributes associated with shape and TSM concentration. The MERIS images comprise a band with the TSM concentration values, which are retrieved through an algorithm carried out by an ANN, trained to emulate the inverse model (Schiller and Doerffer 2005). In previous works on the same study area, it was found that the TSM concentration values provided by MERIS may be considered valid, despite the lack of in situ validation (Teodoro et al. 2009a; Teodoro and Almeida 2011). MERIS images from the year of 2009 were considered to analyze the TSM concentration. Among the 133 available images covering the study area, only 71 MERIS FR scenes (level 2 data) were considered valid for

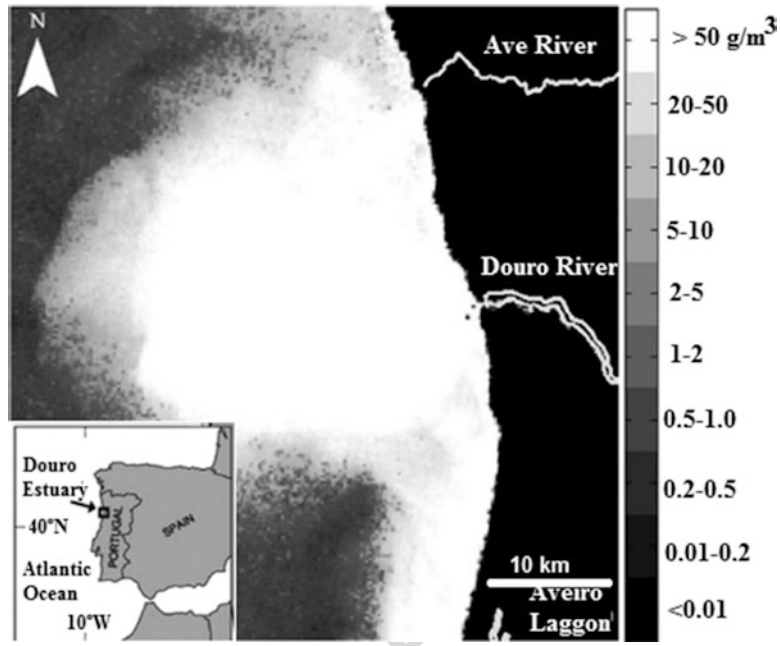

Fig. 3.11 TSM concentration retrieved from first MERIS scene of 8 March 2003 for the study area

the identification of the plume (the others were discarded due the presence of clouds or other atmospherics effects).

Two approaches were employed in order to identify the DRP: manual and automatic. The manual identification of a river plume may become a quite subjective task due to the high degree of subjectivity of human intervention. In order to achieve a basis of comparison and prove the high degree of subjectivity of this approach, a manual identification of the river plume was independently performed by two experienced operators in a GIS environment.

The automatic identification of the DRP was performed through a segmentation approach. In previous works on this subject, it was evidenced that image segmentation methods based on the image domain (pixel values) are more appropriate to extract the river plume from MERIS data than feature-based methods (Teodoro et al. 2009a; Teodoro and Almeida 2011). The region-based approach proposed in Teodoro et al. (2009a) indicated fixed values for the seed (S) and threshold (T) parameters, as they were appropriate for MERIS images with a clear saturation of TSM values in the plume region. In this work, a fully automatic method was considered. Initially, the MERIS images with original TSM concentration values are taken. The advantage of considering the TSM concentration values instead Log_{10} (TSM) relies on a better discrimination of the plume with respect to its surrounding pixels, since the logarithm reduces the separability between the plume and surrounding concentration values. The first step is based on thresholding the image based on a certain cutoff (TSM_{cutoff}), which is associated with the highest correlation between the size of the obtained object (river plume) with the river discharges. It was found that a TSM_{cutoff} equal to 2 is adequate for the study area and its current environment. For other study areas and conditions, a sensitivity analysis on the variation may be performed in order to find the most appropriate value. More details about the sensitivity analysis performed could be founded in Gonçalves et al. (2012). After the thresholding operation, the segmentation result is refined by filling the holes of the detected objects. Finally, the river plume is considered to be the object with the largest area.

A comprehensive characterization of the plume was performed through a set of attributes, which take into account not only the shape of the river plume, but also (Fig. 3.12): size of the

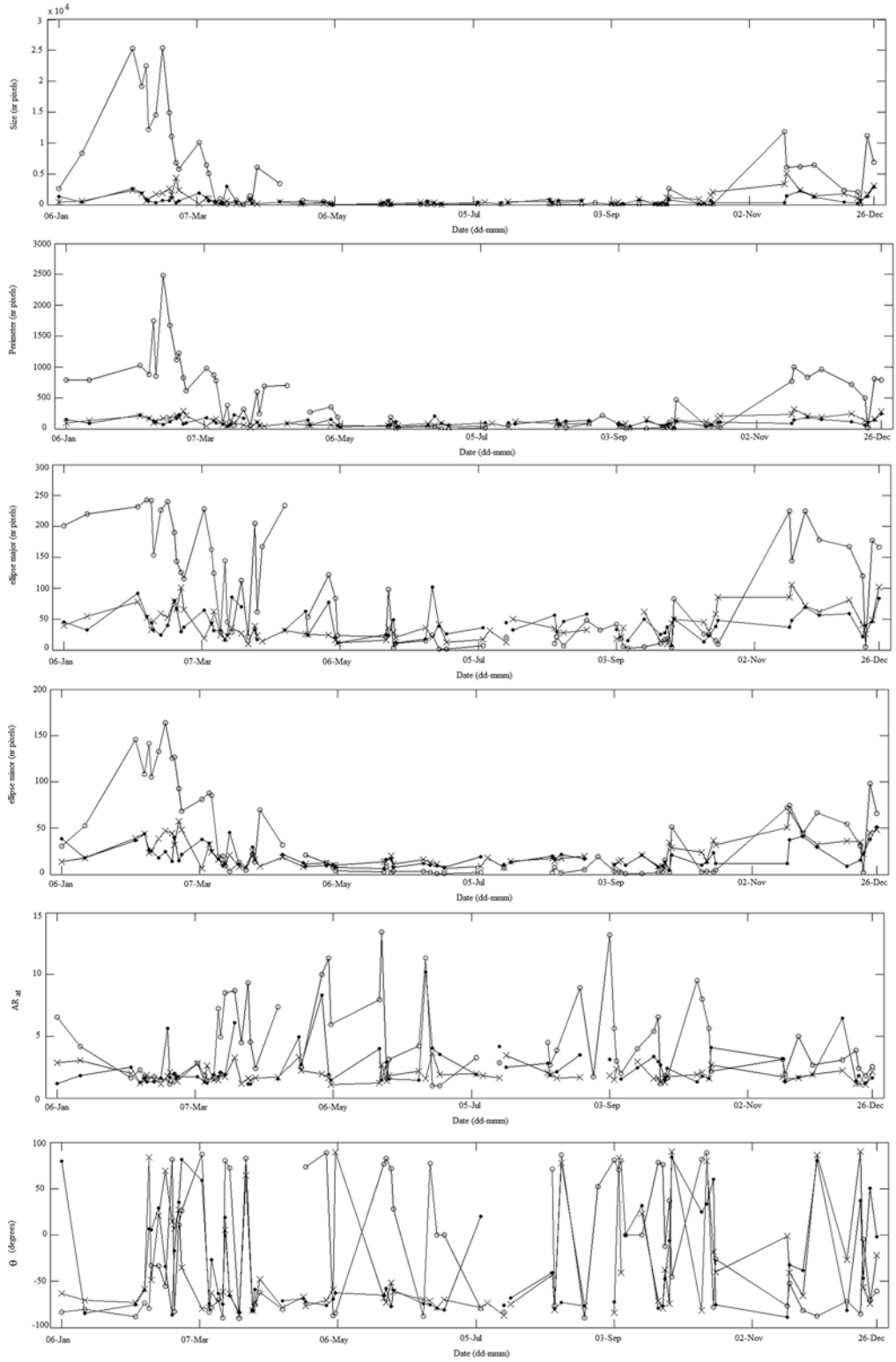

[AU3] **Fig. 3.12** Time-series of the river plume shape attributes Size, Perimeter, ellipse$_{major}$, elippse$_{minor}$, the ratio between ellipse$_{major}$ and elippse$_{minor}$ (AR_{at}) and orientation (θ) pertaining to the manual identification of operator A (.), manual identification of operator B (x) and automatic identification (o) of the river plume (Gonçalves et al. 2012)

plume; perimeter (in number of pixels); the major and the minor axis length of the ellipse adjusted to the river plume; and the orientation, (in degrees). With respect to the TSM concentration values of the pixels within the river plume, the following attributes were considered: average, standard-deviation, maximum, and the sum of all pixel concentrations. Also, in order to relate the plume attributes with environmental parameters, the Douro river discharges (at nearest dam – Crestuma dam), the tide level at Leixões (tide gauge closest to the study area), wind instantaneous speed and wind direction values were considered for the same time.

The results of the manual and automatic procedures are presented and compared. The statistical analysis was based on the bi-dimensional analysis of the variables of this study, and relied on the computation of the Pearson correlation coefficient.

Regarding, the manual identification, the results obtained by the two operators were similar. Among the considered environmental variables, the river discharges presented correlation values above 0.5 with several attributes of the plume. Although moderate, a negative and significant correlation was also found between wind speed and minor axis length of the ellipse adjusted to the river plume, and also between wind speed and the average TSM concentration of the plume.

Considering the automatic plume identification, it was observed that more significant correlation are obtained between environmental variables and river plume attributes than what was observed with the manual procedure. In particular, a moderate yet significant and negative correlation was found between wind speed and perimeter, as well as between wind speed and the major and minor axis of the adjusted ellipse. A high correlation of 0.719 was found between the size of the river plume and the river discharges. The results previously presented suggest that important considerations regarding sedimentary balance can be pointed. It can be observed that the higher river discharges are associated with plumes oriented toward the NW-N direction (corresponding to the range to −45° to −90°). The higher river discharges throw the plume of sediments with more intensity towards east, which then reaches the poleward current and move towards north. The plumes with positive orientation in the range 45–90° (towards the SW-S direction) are mostly associated with lower river discharges and are pushed by the littoral drift current (north-south direction). Focusing on the range of river discharges above 500 m^3/s, the relation between the orientation attribute and the river discharges appear to present a negative exponential decay. These are important considerations which should be taken into account in coastal studies on sedimentary balance and may have important consequences on the natural supply of sediments to feed the beaches of the study area.

Concluding, although MERIS data showed to be a useful data source for the spatio-temporal analysis of the Douro river plume and present a high temporal covarage, other sources of RS data may also be considered in the future. Furthermore, it is necessary to calibrate the reflectance values for TSM concentration values through complex algorithms and also to perform in situ validation. Due the construction of two breakwaters at the mouth of the Douro River (between 2004 and 2008), it is clearly visible that the *output* of sediments into the sea is quite narrower, which means that the TSM concentration values found in the plume are smaller. The objectives of this study were the development of a method for the automatic identification of the Douro river plume from MERIS data, a comprehensive characterization of the river plume, and the spatio-temporal analysis of the river plume and its relation with some environmental variables. The advances in the field achieved by the present work support the interest of further research on this topic, namely the employment of more complex statistical methods and variables to explore other important considerations in this thematic.

3.3.5 Extraction of Estuarine/ Coastal Sandy Bodies

A sand spit is a deposition landform along coasts, mainly caused by dominant littoral drift and wave action. A sand spit does not present a well-

defined topographic boundary, and its boundary is not static in time, as the majority of the water bodies. Moreover, sand spits are influenced by tides, waves and wind. The extraction of a sand spit from a water environment (e.g. an estuary) is a complex task due the presence of bubbles and foam, caused by the breaking waves and the turbidity of the water, which difficult an accurate extraction of the boundary.

One of the major applications of remotely sensed data is change detection. Change detection involves the ability to quantify temporal evolution using multi-temporal data sets. Several works related to the extraction estuarine/coastal landforms from satellite data were referred in the literature. Frihy et al. (1997) used LANDSAT images and topographic maps to study the Damietta promontory of the Nile delta. However, in these works the identification of the coastal landforms was based in visual inspection and false color composition images. Specifically relate to dunes identification/characterization several works were also referred in the literature (e.g. Chowdhury et al. 2011; Sanjeevi 1996). A number of problems in RS require the segmentation of specific spectral classes such as water bodies (e.g. Lira 2006). However, very few works related to the extraction of estuarine/coastal sandy bodies from a water environment from satellite data through segmentation techniques were done. Oliveira et al. (2008) study the geomorphologic evolution of the coastal zone of the Restinga of Marambaia (Brasil) using multitemporal satellite images. The images were segmented by a region growth algorithm and submitted to an unsupervised classification. Silveira and Heleno (2009) proposed an approach for water/land separation in SAR images that uses region-based level sets and adopts a mixture of lognormal densities as the probabilistic model for the pixel intensities in both water and land regions. Teodoro et al. (2011a) and after Teodoro and Gonçalves (2012) present a work that aims to develop and implement an effective and automatic monitoring technique, based on remotely sensed data (IKONOS-2 images) and image processing techniques, in order to accurately extract the sand spit boundary and consequently estimate the sand spit area. The study area selected for this study was the Cabedelo sand spit located in the Douro river estuary (Fig. 3.13). Two thirds of the Douro river mouth is protected by the Cabedelo

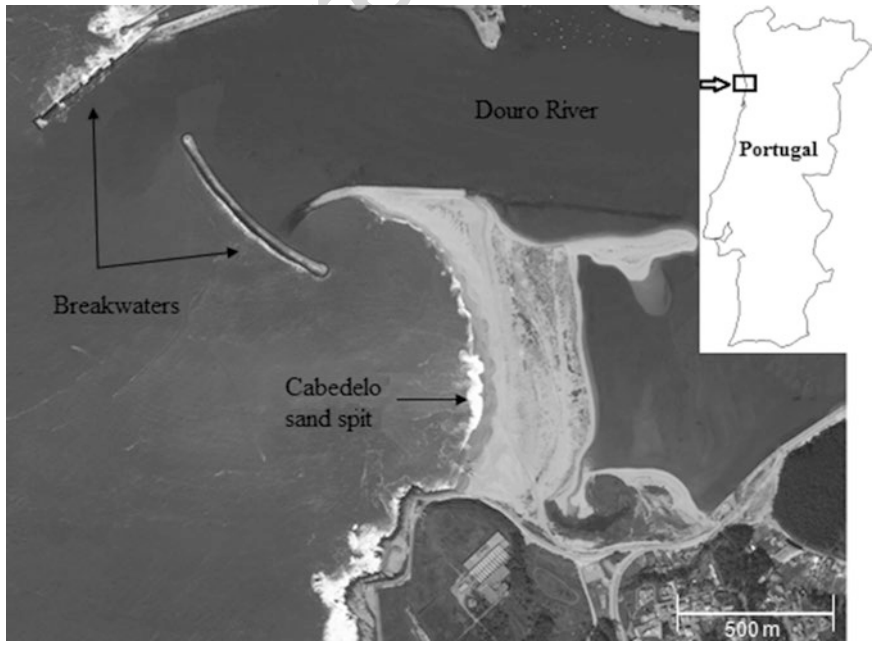

Fig. 3.13 Cabedelo sand spit (Teodoro and Gonçalves 2012)

sand spit, creating a micro-ecosystem of great biological interest. Cabedelo is a very dynamic morphologic structure and is influenced by several dynamic agents such as waves, tides, and wind speed and direction; and acts as a barrier, protecting the estuary banks from waves, especially during storms. In the last decades the protection function of the sand spit has been reduced, especially due to the retreatment to the interior of the estuary. In order to counteract this situation, two breakwaters were constructed to stabilize the river mouth, between 2004 and 2008.

The methodology proposed in Teodoro and Gonçalves (2012) consists in the application of a semi-automatic approach based on segmentation, called GThE (Global Thresholding refined through detected Edges). In order to access the performance of this new approach, the results of the GThE method were compared with pixel-based and OBIA classification algorithms already applied in Teodoro et al. (2011a). It is a requirement of the GThE method that the input image should only comprise, as much as possible, the sand spit and its surroundings. The first step of the GThE methodology is to apply the Otsu's method, which is a nonparametric and unsupervised method of automatic threshold selection for image segmentation (Otsu 1979). The sand spit is frequently still linked to other regions of the image, or to spurious pixels. Therefore, there is the need to perform a refinement on the result of the global thresholding, separating the sand spit from other parts of the image. The second stage of the GThE methodology then consists on the application of the Canny edge detector (Canny 1996). The Canny edge detector, with a standard deviation of the Gaussian filter equal to 0.5, presented better performance. The edges computed by the Canny edge detector are then used on a clipping operation of the previously segmentation obtained on global thresholding. As a final segmentation step, the segmentation is improved by filling the holes of the segmented object (Fig. 3.14).

The GThE methodology is applicable to a single band image. Regarding the IKONOS-2 sensor, the NIR and the panchromatic bands are the most adequate for this approach. The NIR is the spectral band which provides better discrimination between water and land, whereas the use of panchromatic band increases the spatial resolution, and consequently allow for a more accurate delineation of the sand spit boundary. In order to evaluate the performance of the GThE, a pixel-based (supervised classification) and an OBIA classification algorithm were also applied to the six IKONOS-2 images used. The performance of the supervised classifications methods was evaluated through the error matrix and the discrete multivariate Kappa statistic (Story and Congalton 1986; Bishop et al. 1975). The best result was found for the MLC for all the IKONOS-2 images, with an Overall Accuracy (OA) higher than 96.4 % and a kappa-statistic higher than 0.93. The results regarding the OBIA approach were similar to the MLC (pixel-based classification). However, these apparently good results are associated with the pixel classification, which do not necessarily imply an accurate sand spit delineation. One of the main problems addressed in this paper is how to determine the end of the spit. Through the algorithms previously applied the boundary between the main land and the sand spit is well defined both for pixel-based and OBIA classification, as expected. However, a new class (not sand or water) that defines the boundary between the sand spit and the estuary/sea. This fact is justified not only by the presence of bubbles and foam, as well as by the high turbidity of water and consequently a high concentration of TSM, which changes the spectral response of the sea water. This fact justifies the development of this new approach (GThE) in order to accurately extract the sand spit boundary. As already referred, the application of the GThE method has generally led to considerable better results with the panchromatic band. However, it was verified if the fusion of the NIR and panchromatic bands allows for better results. An improvement of the obtained results was verified only for two images (December 2001 and June 2004). However, the remaining images presented a worst performance, which may be explained by the selection of the interpolation method in the fusion process. This aspect deserves further research. The Otsu's method

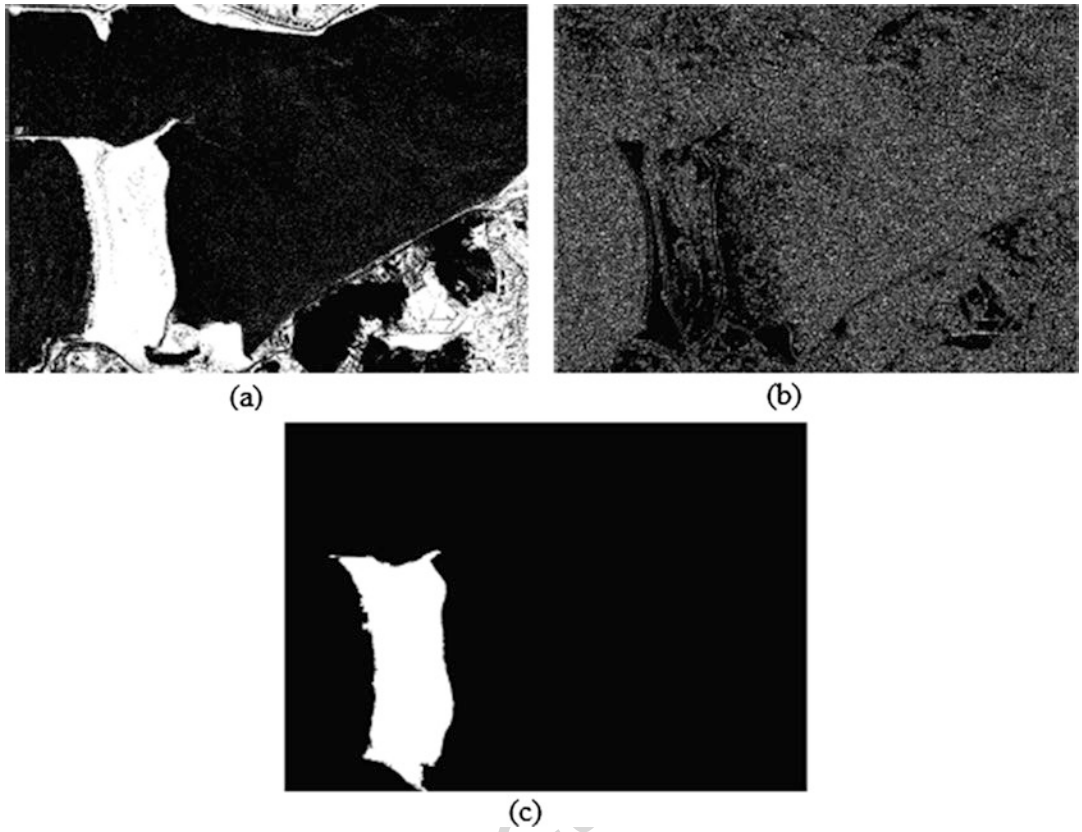

Fig. 3.14 GThE steps. (**a**) Global thresholding of the IKONOS-2 image of June 2004 through the Otsu's method. (**b**) Edges of the same image obtained through the Canny edge detector. (**c**) Final extraction of the sand spit, through the refinement of the global thresholding in (**a**) through the edges represented in (**b**) (Teodoro and Gonçalves 2012)

comprises the computation of an effectiveness metric. A higher separability between the classes of the histogram is associated with a higher between-class variance, and consequently higher values of this effectiveness metric. More details about this metric could be founded in Teodoro and Gonçalves (2012).

In order to evaluate the performance of the three methods used in the estimation of the sand spit area pixel-based, OBIA and GThE, two sets of reference values were used. The first reference set, called manual reference, was based on a manual digitalization on a GIS environment of the sand spits on the IKONOS-2 image, followed by the computation of the non-regular polygon area in the shapefile. The second approach was based on field surveys through differential Global Positioning System (dGPS) processing techniques. The dataset considered in this study consists of six dGPS surveys of discrete points (Baptista et al. 2008). The outland profile network limit is the shoreline defined by the contact between the wave swash and the foreshore. The values were later processed in a GIS environment and linearly interpolated for different tide levels (0, 1 and 2 m). These values were used to estimate the correspondent sand spit area, for the tide level correspondent to each IKONOS-2 image. Analysing the results presented in Table 3.1, the GThE method presented slightly better results than the other methods, with a clear advantage of a considerable faster performance, beyond requiring a minimum operator intervention. Moreover, the GThE method presents consistently better results than considering only the pixel-based or OBIA methods. The relative error decreases from

t4.1 **Table 3.4** Average and standard-deviation (Stdv) of the
t4.2 relative errors (in %), regarding the three methods applied,
t4.3 considering the manual and dGPS reference values

t4.4		Manual reference		DGPS reference	
		Average	Stdv	Average	Stdv
t4.5	Pixel-based[a]	4.1	3.2	6.4	7.4
t4.6	Object-based	2.5	1.2	4.7	5.9
t4.7	GThE	2.4	2.0	4.2	5.0

t4.8 [a]Considering the Maximum Likehood Classification
t4.9 (*MLC*) algorithm

2.4 ± 2.0 to 1.8 ± 1.5 (average ± Stdv) if the image from June 2004 was discarded, where the NIR band was considered instead of the panchromatic band (Table 3.4).

In order to provide a more complete evaluation of GThE performance, three additional attributes were computed on the extracted sand spit: the perimeter, which is obtained by calculating the distance between each adjoining pair of pixels around the border of the sand spit; the ratio between the major and the minor axis length of the ellipse adjusted to the sand spit (ARat); and the fractal dimension (Db) which considers the particular complexity nature of an object shape. Considering the Spearman correlation coefficient and p-value of the nonparametric Mann-Whitney statistical test, it was founded that for the attributes Area and ARat, the GThE method presented similar values to the manual reference. Significant differences were found between GThE and the manual reference regarding the attribute perimeter. Regarding the attribute Db, only significant differences were found between GThE and the manual reference with 4 m pixel size. Significant differences were also found between the manual references with different pixel sizes, both for perimeter and Db attributes, despite presenting high correlation values.

The Cabedelo sand spit responds dynamically to the seasonality of the hydrodynamic cycles with the lower area values occurring in the Winter and the higher area values occurring in Summer (Baptista et al. 2008). However, as in this study the dataset was considerably small, it did not allowed for a time-series analysis and the seasonality tendency could not be proved. However, other important studies may also be performed, namely by investigating the relation of the sand spit instantaneous area with hydrodynamic and agitation variables such as the tide level (TL), wind speed (WS), wind direction and river discharge at the nearest dam (RD) and the significant wave height (Hs). However, in this work, only six images were available, which is a small number to perform a robust statistical study. Therefore, the non-parametric Spearman correlation coefficient was computed between the sand spit area and TL, WS, RD and Hs parameters. The higher correlation coefficient was found between the sand spit area and RD ($r = 0.429$, $p = 0.397$), where the lack of statistical significance is probably related to the small number of available images. This may be due to the fact that the Crestuma dam (nearest dam) controls the fresh water flow into the estuary when the natural flow is less than 7000 m^3/s.

Concluding, the GThE method proposed in this study presented slightly better performance than the two supervised approaches (pixel-based and OBIA classification). Moreover, it presents the advantage of being a fast procedure and with a high potential for a fully automation. This would allow for a more consistent analysis of the sand spit behaviour and evolution across the time. The GThE approach has also the advantage of avoiding in situ surveys, and allows for assessment of historical records through archived satellite data. The extraction of sand spits from remotely sensed data has the disadvantage of being an area estimated for the image instant acquisition. In order to make an effective analysis of the sand spit area evolution with more data, it will be necessary to take into account the hydrodynamic and agitation parameters that influence the Cabedelo area, such as the river discharge, tide level or the significant wave height. Nevertheless this research allows for obtaining data in a simple way, currently nonexistent for the Cabedelo sand spit and offers an effective and accurate methodology for monitoring the Cabedelo sand spit size. This work could also, in the future, contribute to evaluate the behaviour of Douro river mouth breakwaters related with coastal defence and sand spit stabilization.

3.3.6 Beach Features/Patterns Identification

Evaluation of beach hydromorphological behaviour and its classification is highly complex. This complexity results from the interaction between wave climate and solid boundaries (beaches, groins, seawalls, among others), occurrence of dynamic events, nonlinearity of phenomena and interactions, different temporal scales (from seconds to hundreds of years), and difficulty on getting historical data (hydrodynamic, geomorphologic and topographic) reliable and continuous in time. Interface zone (sea/land) presents huge challenges in terms of data collection and monitoring. Beach morphological classification was mainly established for Australian and American microtidal sandy environments, where several beach morphologic and classification models were presented (e.g. Short 1991, 1999, 2006, 2012). These models were mainly based on in situ data (wave, tidal and sediment parameters). Parameters such as those are usually unavailable/non-existent for the Portuguese coastal zone. Therefore, without these parameters, the morphologic analysis remotely sensed data seems to be a good approach to identify and to classify beach morphologies.

RS in general is a very powerful tool for beach monitoring and investigation, since it allows collection of spatially continuous information over a vast area in a short time frame. Cracknell (1999) and subsequently Malthus and Mumby (2003) provided an overview of the capacities of RS for estuarine and coastal zone studies. While the focus in these review articles is mainly on low-resolution RS, Mumby and Edwards (2002) investigated the additional value of VHSR data (IKONOS) and hyperspectral data. More recently, Harris et al. (2011) implemented a methodology in order to classify and map beach morphodynamic types from satellite imagery in order to map beach biodiversity using Google Earth data and SPOT-5 images. Mujabar and Chandrasekar (2012) employed an integrated approach comprising visual image interpretation and MLC supervised classification to classify the coastal landforms features along the southern coastal Tamil Nadu (India) through IRS data. Rodríguez-Martín and Rodríguez-Santalla (2013) used ASTER images to detect the sand bars in the Ebro delta coast. McCarthy and Halls (2014) used WorldView-2, QuickBird, and IKONOS satellite sensors and unsupervised and supervised methods using a variety of spectral band combinations. Light Detection and Ranging (LiDAR) elevation and texture data pan sharpening, and spatial filtering were also tested in order to mapping the coastal area of Masonboro Island (North Carolina, USA).

Pais-Barbosa et al. (2009) presented a methodology to identify, measure and classify hydroforms and hydromorphologies, as well as to classify beach morphological stage on the Portuguese northwest coast, based on the visual analysis of vertical aerial photographs datasets in a GIS environment. However, there are some disadvantages associated to this methodology, such as the time consumption, the subjectivity introduced by the operator, and the impossibility of evaluating the accuracy of the visual analysis. In order to complement and improve the work developed by Pais-Barbosa et al. (2009). Teodoro et al. (2009b, c) presented a new approach where a pixel based classification (supervised or unsupervised) and OBIA approaches were employed. The area selected for this analysis is located on the Portuguese northwest coast. This coastal stretch represents a dynamic and fragile physical and biological environment, which is constantly changing in response to natural processes and human activities. The dataset is composed by two aerial photographs (1996 and 2001) and one IKONOS-2 image (2004). Five training classes were defined: Sea, Rip Currents, Breaking Zone, Beach Face and Beach. All the classes presented a very good separability (>1.9). Three supervised classification algorithms (parallelepiped with MLC as tie breaker, minimum distance and MLC) and two unsupervised classification algorithms (K-Means and ISODATA) were applied to the dataset in order to identify morphological features and hydrodynamic patterns. The same supervised and unsupervised classification algorithms were applied to the IKONOS-2 image. The performance of the OBIA classification for

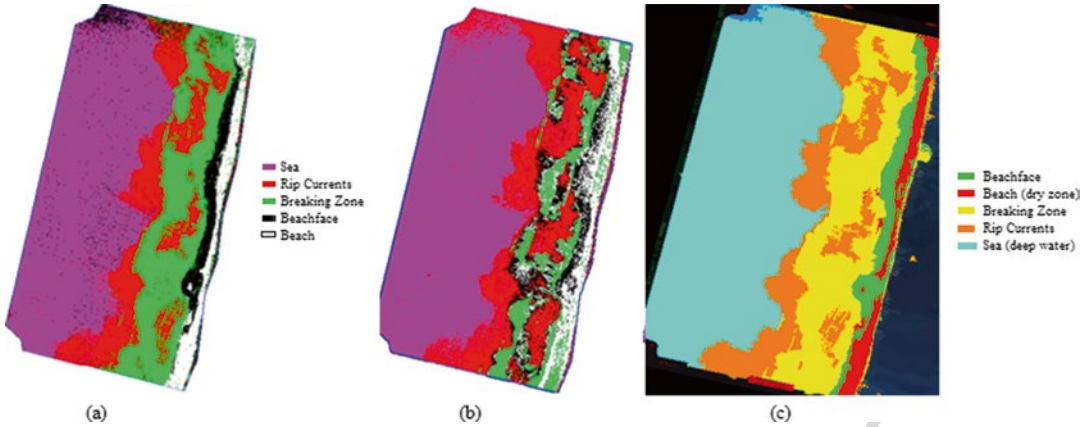

Fig. 3.15 Results of: (**a**) parallelepiped (with MLC as tie breaker); (**b**) K-Means; and **c** object-based classification, for the aerial photograph of 1996 (Adapted from Teodoro et al. 2009b)

the aerial photographs was very good, and allowed to identifying several interest classes, as sea, rip currents, breaking zone, beach face and beach (Fig. 3.15). For the two aerial photographs the best results were found for the MLC, with an OA of 99.28 % and 99.25 % and Kappa coefficient of 0.993 and 0.988 for 1996 and 2001, respectively. Regarding with the IKONOS-2 image the results archived were not so good. The best result was achieved for the 1996 aerial photograph, with an OA of 79.75 % and Kappa coefficient value of 0.728. This fact reduces the OBIA classification performance, classifying objects with similar characteristics in different classes. These results were compared with the visual identification performed by Pais-Barbosa et al. (2009), showing a good agreement between the visual identification and the "automatic" classification (Teodoro et al. 2009b, c).

Later, in order to improve and develop new methodologies to identify coastal features/patterns, Teodoro et al. (2011b) presented a new approach based on Principal Components Analysis and Histogram segmentation (PCAH) aiming to identify and analyze morphological features and hydrodynamic patterns, only applied to the IKONOS-2 image. The main concept relies on Principal Component Analysis (PCA), which allows the information on the n available spectral bands from the image to be combined into an equal number n of principal components (Gonzalez and Woods 2008). In this way, each component is obtained from a linear combination of the n spectral bands, and consequently contains information on all of the spectral bands. A pre-processing stage is performed prior to the PCA, which allows for an enhancement of the image. The pre-processing comprises histogram equalization, followed by Wiener filtering (Lim 1990) using a 3×3 window. The filtering step enables not only a reduction in the spiky aspect of the histogram induced by the histogram equalization but also a slight smoothing of the different hydrodynamic forms/patterns present on the image. Following the pre-processing stage and the principal components computation, a meaningful segmentation of each principal component can be performed independently, using histogram-based segmentation. The segmentation can be performed either manually or automatically. The manual procedure is based on visual identification of classes on the histogram, complemented by visual inspection of the principal component values. The automatic identification of classes in a histogram mainly consists of the detection of significant transitions from positive to negative values in a sequence formed by the consecutive slopes of the histogram. Both manual and automatic approaches were tested in this work. The proportion of variance explained by principal components 1, 2, 3 and 4 were, respectively, 94.5 %, 3.9 %, 1.3 % and 0.3 % (Fig. 3.16).

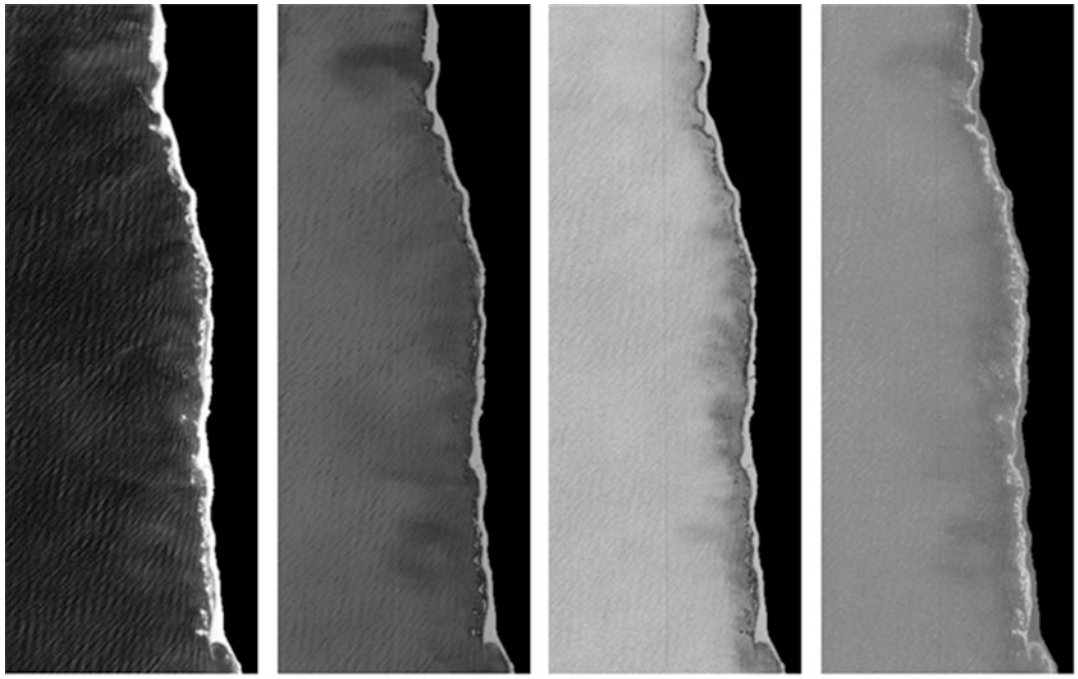

Fig. 3.16 The first (**a**), second (**b**), third (**c**) and fourth (**d**) principal components of the pre-processed IKONOS-2 image (R, G, B and NIR bands) (Teodoro et al. 2011b)

The visual aspect of the principal components is slightly different from what would be expected because of the pre-processing stage that is performed in the PCAH method. The histograms (with both manual and automatic analysis) and resulting segmentations of the principal components obtained were analysed. It was observed that each principal component allows for different identifications of the considered classes. Using the training classes defined for the pixel-based supervised classification, the proportion of correctly classified pixels considering the second principal component were 98 %, 92 %, 43 % and 99 %, for the classes 'sea', 'sediments + breaking zone', 'beach face' and 'beach'. Combining these proportions of agreement with the visual analysis shows that the PCAH method is a promising methodology regarding the identification of beach hydromorphological patterns/forms through remotely sensed data. More details about this method could be founded in Teodoro et al. (2011b).

More recently, Teodoro et al. (2010, 2011c, 2013) and Teodoro (2015) explore the conjugation of high-resolution spatial data combined with data mining techniques to identify/classify beach features/patterns. Different data mining techniques, such as ANN and Decision Trees (DT) have been broadly applied in the field of RS (e.g. Shridhar and Alvarinho 2013; Song et al. 2012). The ANNs have a number of advantages over traditional statistical methods (Wassermann 1989). The ANN can solve nonlinear problems of almost infinite complexity and is more robust in handling noisy and missing data than traditional methods. This is especially desirable for satellite data from visible and infrared sensors that often have a considerable portion of the image not visible because of clouds. Related to ANN, and in a coastal area context, ANN has been used to produce "fuzzy" maps of LULC changes in Mexico (Mas 2004) and wetland vegetation coverage in Florida (Filippi and Jensen 2006). ANN, utilizing a layered thematic classification approach, has

also been used to map coastal Argentina (Kandus et al. 1999) and to examine coastal areas of the Gulf of Mississippi (O'Hara et al. 2003).

The DT algorithm is one of the most popular data mining techniques and has also been applied with success to extract forms/patterns from different types of satellite data. A DT is a classifier expressed as a recursive partition of the instance space. The DT consists of nodes that form a rooted tree, meaning it is a directed tree with a node called root that has no incoming edges. DT learning algorithm is superior to other algorithms in many aspects. It is computationally fast, makes no assumption on data distribution, can attain nonlinear mapping and easily interpretable rules, and has an embedded ability for feature selection (Wang and Li 2008). Saran et al. (2009) presented different approaches to obtain an optimal LULC map based on RS imagery (ASAR and ASTER) for a Himalayan watershed in northern India. A digital classification using MLC and a DT classifier was applied. The results obtained from the DT were better and even improved after post classification sorting. Jin and Mountrakis (2013) performed a case study in Denver (Colorado, USA), where probabilities of urban change generated from two existing urban prediction models (based on DT and logistic regression) are combined as additional information content with a LANDSAT TM scene. Teodoro (2015) developed a recent work related to the application of data mining techniques, particularly ANN and DT, to an IKONOS-2 image (18 September 2008) in order to identify and classify beach features and their geographic patterns and to compare the performance of the ANN and DTs in a particular stretch of the northwest coast of Portugal (limited to the north by the Douro River mouth (Porto city) and to the south by a small fishing village (Aguda), with an extension of approximately 9.5 km). Despite the fact that ANN and DT are well-known classifications methods in the classification of VHSR data, they are not usually applied in the identification/classification of beach features/patterns. Based on the knowledge of the coastal features (Teodoro et al. 2011b) the same five training classes were considered: Sea (S), Suspended-Sediments (SS), Breaking-Zone (BZ), Beach Face (BF), and Beach (B). The dataset was composed of 13 775 pixels unequally comprising the five classes (Teodoro et al. 2010). Each pixel is associated with the reflectance of each spectral band (blue, green, red, and NIR) and the corresponding class. The dataset was randomly divided into training (70 % of each class) and validation (30 % of each class) subsets.

The ANN used in this study consisting of four input nodes, ten hidden nodes (one hidden layer), and five output nodes. The weights of the ANN were estimated based on the back-propagation algorithm (Haykin 1999). The *nnet* package (Ripley and Venables 2014) available in R software (R Core Team 2013) was used. The network performance was assessed by estimating the accuracy with which the validation data were classified. The OA was equals to 98.6 % and the Kappa coefficient equals to 0.97.

The DT used in this work was implemented through the *rpart* package found in the R software (R Core Team 2013), that includes a set of routines related to many of the ideas found in the Classification And Regression Tree (CART) book and programs implemented by Breiman et al. (1984). The tree is built by the following process: first the single variable which best splits the data into two groups is found. After the data are separated, then this process is applied separately to each subgroup, and so on recursively until the subgroups either reach a minimum size or until no improvement can be made. The second stage of the procedure consists of using cross-validation to trim back the full tree. Cost-complexity pruning of the *rpart* routines determines a nested sequence of subtrees of the supplied *rpart* object by recursively snipping off the least important splits based on the threshold complexity parameter (*cp*). More information about the *rpart* package can be found in Therneau and Atkinson (1997). Two DT were developed. The first DT (unpruned) obtained comprises a total of 32 nodes. The OA and Kappa coefficient obtained were very good, presented values higher than 98 % and 0.97 %, respectively. The class that presented the lowest value of the producer accuracy was the "BZ," which was already

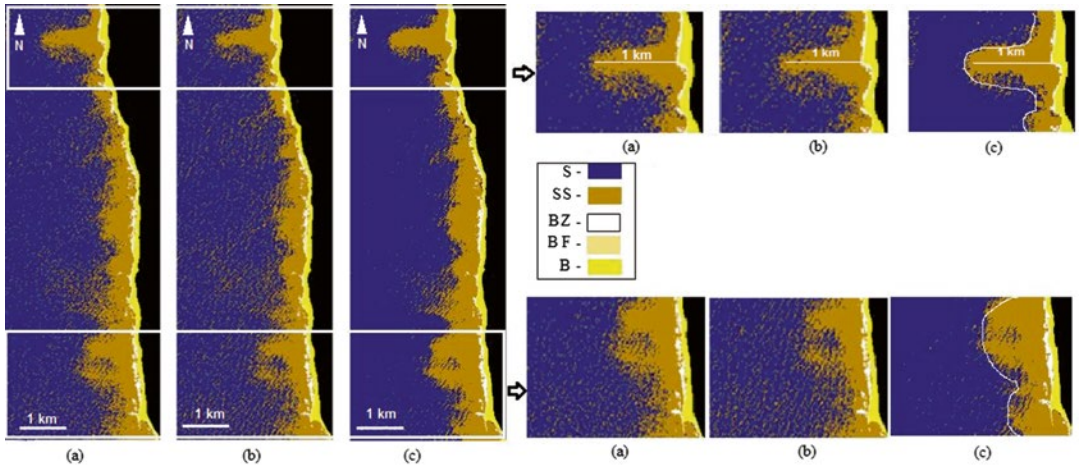

Fig. 3.17 Beach patterns/forms identification and two zoomed areas obtained through: (**a**) DT without pruning; (**b**) DT with pruning (cp = 0.01 e xval = 5); (**c**) ANN (Teodoro 2015)

expected due to its high spectral variability. A second DT was obtained after pruning the original tree, resulting in seven nodes. After pruning the classifier loses some accuracy and sensibility (OA and Kappa values of 96.9 % and 0.950 %, respectively). It is also important to note that for the DT unpruned, the "BF" class presents a user accuracy of 89.5 %, which is the lowest value.

The beach features/patterns identification through an ANN presented accuracies identical to DTs (without pruning the tree), with an OA of 98.6 %. The ANN presented a classification more sensitive to rip currents where pixels belonging to the class "SS" are not incorrectly classified as "S" class. This is visible in the images presented in Fig. 3.17.

The accurate identification of rip currents location, spacing, persistence, and size is of extreme importance for coastal and marine researchers. The data mining algorithms employed in this work (DT and ANN) conduced to better results than the traditional classification methodologies. For the same dataset, the best result for the supervised classifications was achieved with the parallelepiped classifier, with a value of 97 % for OA (Teodoro et al. 2011b). The better result using an OBIA approach was found for the pan-sharpened true colour imagery with an OA not higher than 66 %. Moreover, the rip currents were not clearly identified. This research demonstrated that the association of remotely sensed high-spatial resolution data and data mining algorithms is an effective methodology to identify beach patterns/forms.

3.4 Discussion

Different methods in RS for determining the effect of spatial resolution on marine and coastal ecosystems using different spatial, spectral and temporal resolution images can be applied. The case studies presented here address three main image classification techniques (Pixel-Based (Supervised and Unsupervised) and OBIA classification) and data mining algorithms to evaluate the changes and integrity (health) of the coastal lagoon habitats; to mapping the spatial distribution of natural habitats; to retrieve the TSM concentration; to identify and characterize river plumes; to extract estuarine/coastal sandy bodies; and to identify beach features/patterns.

Making the right decision about which spatial resolution is optimal for the assessment of marine and coastal ecosystems is not an easy matter. First, high spatial resolution images are more detailed than the low spatial resolution images. Second, some features can be identified clearly in high special resolution whereas some features can be recognized in low or moderate spatial res-

olution much clearer. Finally, the coverage using high spatial resolution is smaller than the coverage that introduced by using low spatial resolution images. Therefore, the definition of a precise spatial and temporal resolution depends on the objectives of the research.

As stated before, the advantage of OBIA over pixel-based image analysis is clear when images with high spatial resolution are used. Indeed, in such a case, the increase of the number of spectral bands creates uncertainty in traditional pixel-based classifiers, while by OBIA it was possible to group pixel with similar spectral information into objects. In the case of imagery with medium to low spatial resolution, these enclose lower spectral variability and so are easily handled by pixel-based methods.

[AU4]

For instance, several factors which influence classification accuracy must be considered, such as image data quality, the reliability of training and testing data and the accuracy assessment method. Enhanced efforts are required on the investigation of advanced algorithms and promote a higher usage of hyperspectral imagers and calibrated ship samples to identify accurately the effect of spatial resolution on the accuracy of thematic classifications, and support a better definition of the optimal resolution of remotely-sensed digital data for marine and coastal ecosystems.

3.5 Conclusions

This chapter has illustrated several characteristics of the RS of marine and coastal ecosystems, including its challenges. RS is presented as a powerful marine and costal assessment tool for the shortcoming and future, generating vast quantities of data on spatial and temporal scales heretofore unimaginable, and allowing the development of new image processing algorithms. It now appears that RS needs, cost and technology are converging in a way that will prove practical and cost-effective for marine and costal managers and researchers. Finally, to draw conclusions about marine and coastal assessment, it is essential to develop both a near real-time RS system, which includes more accurate ground truth information, for the marine and coastal areas and a structure for the distribution of the gathered information (e.g. as Copernicus services) to managers and researchers. Even with these drawbacks, marine and coastal RS's future is promising.

Acknowledgements The authors wish to thank the General Directorate for the Territory (DGT) for supporting the research under the FIGGIE Program.

The GeoEye Foundation and Digital Globe for explicitly permitting use free-of-charge the satellite images.

The European Space Agency (ESA) for providing the MERIS data and IKONOS-2 images.

Finally, we should like to thank very much all those who have helped draft this chapter.

References

Aagaard T, Black KP, Greenwood B (2002) Cross-shore suspended sediment transport in the surf zone: a field-based parameterization. Mar Geol 185(3/4):283–302

Aguirre-Gomez R (2000) Detection of total suspended sediments in the North Sea using AVHRR and ship data. Int J Remote Sens 21(8):1583–1596

Aplin P (2005) Remote sensing: ecology. Prog Phys Geogr 29(1):104–113. doi:10.1191/030913305pp437pr

Baatz M, Schäpe A (2000) Multiresolution segmentation – an optimization approach for high quality multi-scale image segmentation. In: Strobl J et al (eds) Angewandte Geographische Informationsverarbeitung, XII. Wichmann, Heidelberg, pp 12–23

Baatz M, Benz U, Dehghani S, Heynen M, Holtje A, Hofmann P, Lingenfelder I, Mimler M, Sohlbach M, Weber M, Willhauck G (2001) eCognition objectoriented image analysis, V.2.2 user guide. Definiens Imaging, Munchen

Baptista P, Bastos L, Bernardes C, Cunha T, Dias J (2008) Monitoring sandy shores morphologies by DGPS – a practical tool to generate digital elevation models. J Coastal Res 24(6):1516–1528

Bird E (2008) Coastal geomorphology: an introduction, 2nd edn. Wiley, England

Bishop Y, Fienberg S, Holland P (1975) Discrete multivariate analysis: theory and practice. MIT, Cambridge, MA

Blaschke T, Lang S (2006) Object based image analysis for automated information extraction – a synthesis. In: Abstracts of the measuring the earth II ASPRS fall conference, San Antonio, 6–10 Nov 2006

Blaschke T, Lang S, Hay GJ (2008) Object-based image analysis: spatial concepts for knowledge-driven remote sensing applications. Springer, Berlin

Bock M, Rossner G, Wissen M, Remm K, Langanke T, Lang S, Klug H, Blaschke T, Vrscaj B (2005a) Spatial

indicators for nature conservation from European to local scale. Ecol Indic 5:322–338

Bock M, Xofis P, Mitchley J, Rossner G, Wissen M (2005b) Object oriented methods for habitat mapping at multiple scales – case studies from northern Germany and Wye Downs, UK. J Nat Conserv 13:75–89

Breiman L, Friedman JH, Olshen RA, Stone CI (1984) Classification and regression trees, Wadsworth statistics/probability series, 1st edn. Chapman and Hall/CRC, New York

Buiten HJ, Clevers JGPW (1990) Remote sensing, theorie en toepassingen van landobservatie (Remote sensing theory and applications of land observation). Pudoc, Wageningen

Bustamante J, Pacios F, Díaz-Delgado R, Aragonés D (2006) Predictive models of turbidity and water depth in the Doñana marshes using Landsat TM and ETM+ images. In: Proceedings of the first international symposium on GlobWetlands: looking at wetlands from space, SP-634, ESA/ESRIN, Frascati, 19–20 Oct 2006

Bustamante J, Díaz-Delgado R, Aragonés D, García Murillo P, Castellanos EM et al (2013) Proyecto HYDRA: aplicación de la teledetección al estudio de la dinámica hídrica y de la vegetación acuática en las marismas de Doñana. In: Fernández-Renau González-Anleo A, de Miguel Llanes E (eds) Teledetección: Sistemas Operacionales de Observación de la Tierra. XV Congreso de la Asociación Española de Teledetección (AET). Torrejón de Ardoz, Madrid, España, 22–24 Oct 2013

Canny J (1986) A computational approach to edge-detection. IEEE Trans Pattern Anal 8(6):679–698

Chavez PS Jr (1988) An improved dark-object subtraction technique for atmospheric scattering correction of multispectral data. Remote Sens Environ 24:459–479

Chen J, D'Sa E, Cui T, Zhang X (2013) A semi-analytical total suspended sediment retrieval model in turbid coastal waters: a case study in Changjiang River Estuary. Opt Express 21(11):13018–13031

Chen J, Cui T, Qiu Z, Lin C (2014) A three-band semi-analytical model for deriving total suspended sediment concentration from HJ-1A/CCD data in turbid coastal waters. ISPRS J Photogramm 93:1–13

Chowdhury PR, Deshmukh B, Goswami AK, Prasad SS (2011) Neural network based dunal landform mapping from multispectral images using texture features. IEEE J Sel Top Appl 4(1):171–184

Correia MJ, Costa JL, Chainho P, Félix PM, Chaves ML, Medeiros JP, Silva G, Azeda C, Tavares P, Costa A, Costa AM, Bernardo J, Cabral HN, Costa MJ, Cancela da Fonseca L (2012) Inter-annual variations of macrobenthic communities over three decades in a landlocked coastal lagoon (Santo André, SW Portugal). Estuar Coast Shelf Sci 110:168–175. doi:10.1016/j.ecss.2012.04.028

Cracknell AP (1999) Remote sensing techniques in estuaries and coastal zones – an update. Int J Remote Sens 19(3):485–496

Daya-Sabar BS, Ghandi G, Prakasa-Rao BS (1995) Applications of mathematical morphology in surface water body studies. Int J Remote Sens 16:1495–1502

Diaz Varela RA, Ramil Rego P, Calvo Iglesias S, Muñoz Sobrino C (2008) Automatic habitat classification methods based on satellite images: a practical assessment in the NW Iberia coastal mountains. Environ Monit Assess 144:229–250

Digital Globe (2010) The benefits of the eight spectral bands of WorldView-2 (White paper "WP-8SPEC Rev 01/13"). Digital Globe, Colorado

Doeffer R, Fischer J, Stössel M, Brockman C (1989) Analysis of Thematic Mapper data for studying the suspended matter distribution in the coastal area of the German bight (North Sea). Remote Sens Environ 28:61–73

Doxaran D, Froidefond JM, Lavender S, Castaing P (2002) Spectral signature of highly turbid waters: application with SPOT data to quantify suspended particulate matter concentrations. Remote Sens Environ 81(1):149–161

Druon JN, Schrimpf W, Dobricic S, Stips A (2004) Comparative assessment of large-scale marine eutrophication: North Sea area and Adriatic Sea as case studies. Mar Ecol-Prog Ser 272:1–23

Dzwonkowski B, Yan XH (2005) Tracking of a Chesapeake Bay estuarine outflow plume with satellite-based ocean color data. Cont Shelf Res 25:1942–1958

Evans D (2006) The habitats of the European union habitats directive. Biol Environ 106B(3):167–173. doi:10.3318/BIOE.2006.106.3.167

FAO (2014) The state of world fisheries and aquaculture, opportunities and challenges 2014. FAO Report, Rome

Fernández-Nóvoa D, Mendes R, deCastro M, Dias JM, Sánchez-Arcilla A, Gómez-Gesteira M (2015) Analysis of the influence of river discharge and wind on the Ebro turbid plume using MODIS-Aqua and MODIS-Terra data. J Mar Syst 142:40–46

Filippi AM, Jensen JR (2006) Fuzzy learning vector quantization for hyperspectral coastal vegetation classification. Remote Sens Environ 100(4):512–530

Foody GM (2002) Status of land cover classification accuracy assessment. Remote Sens Environ 80(1):185–201. doi:10.1016/S0034-4257(01)00295-4

Forget P, Ouillon S (1998) Surface suspend matter off the Rhone river mouth from visible satellite imagery. Oceanol Acta 21(6):739–749

Förster M, Frick A, Walentowski H, Kleinschmit B (2008) Approaches to utilising QuickBird data for the monitoring of NATURA 2000 habitats. Community Ecol 9:155–168

Freitas MC, Andrade C, Ferreira T, Cruces A, Araújo MF (2007) Wet dune slacks, sea-level and coastal evolution in the southwestern Portuguese façade. J Coastal Res SI 50:231–236

Frick A, Weyer G, Kenneweg H, Kleinschmit B (2005) A knowledge based approach to vegetation monitoring with Quickbird imagery. In: Proceedings of the ISPRS

workshop 2005: high-resolution earth imaging for geospatial information, Hannover, 17–20 May 2005

Frihy OE, Dewidar KM, Nasr SM, El Raey MM (1998) Change detection of the northeastern Nile Delta of Egypt: shoreline changes, Spit evolution, margin changes of Manzala lagoon and its islands. Int J Remote Sens 19(10):1901–1912

Gan TY, Kalinga OA, Ohgushi K, Araki H (2004) Retrieving seawater turbidity from Landsat TM data by regressions and an artificial neural network. Int J Remote Sens 25(21):4593–4615

Gao Y, Mas JF (2008) A comparison of the performance of pixel-based and object-based classifications over images with various spatial resolutions. In: Hay GJ, Blaschke T, Marceau D (eds) GEOBIA 2008 – Pixels, objects, intelligence, GEOgraphic object based image analysis for the 21st century, Calgary, Alberta, Canada, 5–8 Aug 2008. ISPRS Archives, vol XXXVIII-4/C1, p 6

Godin DG, Huan L, Fraser RN, Rundquist DC, Stebbins WA (1993) Analysis of suspended solids in water using remotely sensed high resolution derivative spectra. Photogramm Eng Remote S 9(4):505–510

Gonçalves H, Teodoro AC, Almeida H (2012) Identification, characterization and analysis of the Douro river plume from MERIS data. IEEE J Sel Top Appl 5(5):1553–1563

Gonzalez RC, Woods RE (2008) Digital image processing, 3rd edn. Prentice Hall, Upper Saddle River

Groom G, Mücher CA, Ihse M, Wrbka T (2006) Remote sensing in landscape ecology: experiences and perspectives in a European context. Landsc Ecol 21:391–408. doi:10.1007/s10980-004-3164-9

Gross JE, Goetz SJ, Cihlar J (2009) Application of remote sensing to parks and protected area monitoring: introduction to the special issue. Remote Sens Environ 113(7):1343–1345. doi:10.1016/j.rse.2008.12.013

Guneroglu A, Karsli F, Dihkan M (2013) Automatic detection of coastal plumes using Landsat TM/ETM+ images. Int J Remote Sens 34(13):4702–4714. doi:10.1080/01431161.2013.782116

Gutierres F (2014) Structure and dynamics of habitats and landscape of Sado Estuary and Comporta/Galé Natura 2000 Sites – A contribution to sustainable land management and ecological restoration. Ph.D. dissertation, Institute of Geography and Territorial Planning, University of Lisbon

Gutierres F, Reis E, Neto C, Costa JC, Godinho-Ferreira P (2013) Integrating remote sensing in Natura 2000 habitat monitoring. In: Taveira Pinto F (ed) Proceedings of the 4rd international seminar "Os Recursos Hídricos, o Mar e o Litoral", Porto, 2013. APRH, pp 54–63. ISBN:978-989-8509-09-3

Haest B, Thoonen G, Vanden Borre J, Spanhove T, Delalieux S, Bertels L, Kooistra L, Mücher CA, Scheunders P (2010) An object-based approach to quantity and quality assessment of heathland habitats in the framework of natura 2000 using hyperspectral airborne ahs images. In: Addink EA, Van Coillie FMB (eds) GEOBIA 2010: geographic object-based image analysis, Ghent, 29 Jun–2 Jul 2010. ISPRS Archives, vol XXXVIII-4/C7, p 6

Hall O, Hay GJ, Bouchard A, Marceau DJ (2004) Detecting dominant landscape objects through multiple scales: an integration of object-specific methods and watershed segmentation. Landsc Ecol 19(1):59–76. doi:10.1023/B:LAND.0000018371.43447.1f

Harris L, Nel R, Schoeman D (2011) Mapping beach morphodynamics remotely: a novel application tested on south African sandy shores. Estuar Coast Shelf Sci 92(1):78–89. doi:10.1016/j.ecss.2010.12.013

Hay G, Castilla G (2006) Object-based image analysis: strengths, weaknesses, opportunities and threats (SWOT). In: Lang S, Blaschke T, Schöpfer E (eds) Bridging remote sensing and GIS. 1st international conference on object-based image analysis (OBIA 2006), Salzburg University, Austria, 4–5 Jul 2006. ISPRS Archives, vol XXXVI-4/C42, p 3

Hay GJ, Castilla G (2008) Geographic object-based image analysis (GEOBIA): a new name for a new discipline. In: Lang S, Hay G, Blaschke T (eds) Object based image analysis. Springer, Berlin, pp 75–89

Hay GJ, Blaschke T, Marceau DJ, Bouchard A (2003) A comparison of three image-object methods for the multiscale analysis of landscape structure. ISPRS J Photogramm 57(5–6):327–345

Haykin S (1999) Neural networks: a comprehensive foundation, 2nd edn. Prentice Hall, Upper Saddle River

Hellweger FL, Schlosser P, Lall U, Weissel JK (2004) Use of satellite imagery for water quality studies in New York Harbor. Estuar Coast Shelf Sci 61(3):437–448. doi:10.1016/j.ecss.2004.06.019

Hendiarti N, Siegel H, Ohde T (2004) Investigation of different coastal processes in Indonesian waters using SeaWiFS data. Deep-Sea Res PT II 31(1–3):85–97. doi:10.1016/j.dsr2.2003.10.003

Hu CM, Muller-Karger FE, Biggs DC, Carder KL, Nababan B, Nadeau D, Vanderbloemen J (2003) Comparison of ship and satellite bio-optical measurements on the continental margin of the NE Gulf of Mexico. Int J Remote Sens 24(13):2597–2612. doi:10.1080/0143116031000067007

Islam MR, Yamaguchi Y, Ogawa K (2001) Suspended sediment in the Ganges and Brahmaputra Rivers in Bangladesh: observation from TM and AVHRR data. Hydrol Process 15(3):493–509. doi:10.1002/hyp.165

Jiang L, Yan X-H, Klemas V (2009) Remote sensing for the identification of coastal plumes: case studies of Delaware Bay. Int J Remote Sens 30(8):2033–2048. doi:10.1080/01431160802549211

Jin H, Mountrakis G (2013) Integration of urban growth modelling products with image-based urban change analysis. Int J Remote Sens 34(15):5468–5486. doi:10.1080/01431161.2013.791760

Kandus P, Karszenbaum H, Frulla L (1999) Land cover classification system for the lower delta of the Parana river (Argentina): its relationship with landsat thematic mapper spectral classes. J Coastal Res 15(4):909–926

Kennedy RE, Townsend PA, Gross JE, Cohen WB, Bolstad P, Wang YQ, Adams P (2009) Remote sensing

change detection tools for natural resource managers: understanding concepts and tradeoffs in the design of landscape monitoring projects. Remote Sens Environ 113(7):1382–1396. doi:10.1016/j.rse.2008.07.018

Keramitsoglou I, Kontoes C, Sifakis N, Mitchley J, Xofis P (2005) Kernel based re-classification of earth observation data for fine scale habitat mapping. J Nat Conserv 13(2–3):91–99. doi:10.1016/j.jnc.2005.02.004

Kerr JT, Ostrovsky M (2003) From space to species: ecological applications of remote sensing. Trends Ecol Evol 18(6):299–305. doi:10.1016/S0169-5347(03)00071-5

Klemas V (2011) Remote sensing techniques for studying coastal ecosystems: an overview. J Coastal Res 27(1):2–17, doi:http://dx.doi.org/10.2112/JCOASTRES-D-10-00103.1

Kutser T, Metsamaa L, Strömbeck N, Vahtmäe E (2006) Monitoring cyanobacterial blooms by satellite remote sensing. Estuar Coast Shelf Sci 67(1–2):303–312. doi:10.1016/j.ecss.2005.11.024

Lang S (2008) Object-based image analysis for remote sensing applications: modeling reality – dealing with complexity. In: Lang S, Hay G, Blaschke T (eds) Object based image analysis. Springer, Berlin, pp 3–27

Lang S, Blaschke T (2003) Hierarchical object representation – comparative multi-scale mapping of anthropogenic and natural features. In: Ebner H, Heipke C, Mayer H, Pakzad K (eds) IC II/IV, WG III/4, III/5, III/6 photogrammetric image analysis, Munich, 17–19 Sept 2003. ISPRS Archives, vol XXXIV-3/W8, p 6

Lechner AM, Stein A, Jones SD, Ferwerda JG (2009) Remote sensing of small and linear features: quantifying the effects of patch size and length, grid position and detectability on land cover mapping. Remote Sens Environ 113(10):2194–2204. doi:10.1016/j.rse.2009.06.002

Lengyel S, Déri E, Varga Z, Horváth R, Tóthmérész B, Henry PY, Kobler A, Kutnar L, Babij V, Seliškar A, Christia C, Papastergiadou E, Gruber B, Henle K (2008) Habitat monitoring in Europe: a description of current practices. Biodivers Conserv 17(14):3327–3339. doi:10.1007/s10531-008-9395-3

Liew SC, Saengtuksin B, Kwoh LK (2011) Mapping water quality of coastal and inland waters using high resolution WorldView-2 satellite imagery. In: Proceedings of the 34th international symposium on remote sensing of environment, Sydney, 10–15 Apr 2011

Lillesand TM, Kiefer RW, Chipman JW (2008) Remote sensing and image interpretation, 6th edn. Wiley, Hoboken

Lim JS (1990) Two-dimensional signal and image processing. Prentice Hall, Upper Saddle River

Lira J (2006) Segmentation and morphology of open water bodies from multispectral images. Int J Remote Sens 27(18):4015–4038. doi:10.1080/01431160600702384

Lira J, Morales A, Zamora F (1997) Study of sediment distribution in the area of the Panuco river plume by means of remote sensing. Int J Remote Sens 18(1):171–182. doi:10.1080/014311697219349

Malthus TJ, Mumby PJ (2003) Remote sensing of the coastal zone: an overview and priorities for future research. Int J Remote Sens 24(13):2805–2815. doi:10.1080/0143116031000066954

Mas JF (2004) Mapping land use/cover in a tropical coastal area using satellite sensor data, GIS and artificial neural networks. Estuar Coast Shelf Sci 59(2):219–223. doi:10.1016/j.ecss.2003.08.011

McCarthy MJ, Halls JN (2014) Habitat mapping and change assessment of coastal environments: an examination of WorldView-2, QuickBird, and IKONOS satellite imagery and airborne LiDAR for mapping barrier island habitats. ISPRS Int J Geo-Inf 3(1):297–325. doi:10.3390/ijgi3010297

McFeeters SK (1996) The use of the Normalized Difference Water Index (NDWI) in the delineation of open water features. Int J Remote Sens 17(7):1425–1432. doi:10.1080/01431169608948714

Mehner H, Cutler M, Fairbairn D, Thompson G (2004) Remote sensing of upland vegetation: the potential of high spatial resolution satellite sensors. Global Ecol Biogeogr 13:359–369. doi:10.1111/j.1466-822X.2004.00096.x

Mendes R, Vaz N, Fernández-Nóvoa D, da Silva JCB, de Castro M, Gómez-Gesteira M, Dias JM (2014) Observation of a turbid plume using MODIS imagery: the case of Douro estuary (Portugal). Remote Sens Environ 154:127–138. doi:10.1016/j.rse.2014.08.003

Mertes LAK, Warrick JA (2001) Measuring flood output from 110 coastal watersheds in California with field measurements and SeaWiFS. Geology 29(7):659–662. doi:10.1130/0091-7613(2001)029<0659:MFOFCW>2.0.CO;2

Miller RL, Mckee BA (2004) Using MODIS Terra 250 m imagery to map concentration of total suspended matter in coastal waters. Remote Sens Environ 93(1–2):259–266. doi:10.1016/j.rse.2004.07.012

Mücher CA (2009) Geo-spatial modeling and monitoring of European landscapes and habitats using remote sensing and field surveys. Ph.D. dissertation, Wageningen University

Mücher CA, Kooistra L, Vermeulen M, Haest B, Spanhove T, Delalieux S, Vanden Borre J, Schmidt A (2010) Object identification and characterization with hyperspectral imagery to identify structure and function of NATURA 2000 habitats. In: Proceedings of the Geobia conference, Ghent, 30 June–2 July 2010

Mujabar PS, Chandrasekar N (2012) Dynamics of coastal landform features along the southern Tamil Nadu of India by using remote sensing and geographic information system. Geocarto Int 27(4):347–370. doi:10.1080/10106049.2011.638988

Mumby PJ, Edwards AJ (2002) Mapping marine environments with IKONOS imagery: enhanced spatial reso-

lution can deliver greater thematic accuracy. Remote Sens Environ 82(2–3):248–257. doi:10.1016/S0034-4257(02)00041-X

Myint SW, Walker ND (2002) Quantification of surface suspended sediments along a river dominated coast with NOAA AVHRR and SeaWiFS measurements: Louisiana, USA. Int J Remote Sens 23(16):3229–3249. doi:10.1080/01431160110104700

Nagendra H (2001) Using remote sensing to assess biodiversity. Int J Remote Sens 22(12):2377–2400. doi:10.1080/01431160117096

Nechad B, Ruddick KG, Park Y (2010) Calibration and validation of a generic multisensor algorithm for mapping of total suspended matter in turbid waters. Remote Sens Environ 114(4):854–866. doi:10.1016/j.rse.2009.11.022

Nezlin NP, DiGiacomo PM, Stein ED, Ackerman D (2005) Storm water runoff plumes observed by SeaWiFS radiometer in the Southern California Bight. Remote Sens Environ 98(4):494–510. doi:10.1016/j.rse.2005.08.008

O'Hara CG, King JS, Cartwright JH, King RL (2003) Multitemporal land use and land cover classification of urbanized areas within sensitive coastal environments. IEEE Trans Geosci Remote Sens 41(9):2005–2014. doi:10.1109/TGRS.2003.816573

Oliveira FSC, Kampel M, Amaral S (2008) Multitemporal assessment of the geomorphologic evolution of the Restinga of Marambaia, Rio de Janeiro, Brazil. Int J Remote Sens 29(19):5585–5594. doi:10.1080/01431160802061696

Ondrusek M, Stengel E, Kinkade CS, Vogel RL, Keegstra P, Hunter C, Kim C (2012) The development of a new optical total suspended matter algorithm for the Chesapeake Bay. Remote Sens Environ 119:243–254. doi:10.1016/j.rse.2011.12.018

Otero MP, Siegel DA (2004) Spatial and temporal characteristics of sediment plumes and phytoplankton blooms in the Santa Barbara Channel. Deep Sea Res Part 2 Top Stud Oceanogr 51(10–11):1129–1149. doi:10.1016/j.dsr2.2004.04.004

Otero P, Ruiz-Villarreal M, Peliz A (2008) Variability of river plumes off Northwest Iberia in response to wind events. J Mar Syst 72(1–4):238–255. doi:10.1016/j.jmarsys.2007.05.016

Otero P, Ruiz-Villarreal M, Peliz A (2009) River plume fronts off NW Iberia from satellite observations and model data. ICES J Mar Sci 66(9):1853–1864. doi:10.1093/icesjms/fsp156

Otsu N (1979) A threshold selection method from gray-level histogram. IEEE T Syst Man Cybern 9(1):62–66

Ouillon S, Forget P, Froidefond J-M, Naudin J-J (1997) Estimating suspended matter concentrations from SPOT data and from field measurements in the Rhône River Plume. Mar Technol Soc J 31(2):15–20

Ouillon S, Douillet P, Petrenko A, Neveux J, Dupouy C, Froidefond J-M, Andréfouët S, Muñoz-Caravaca A (2008) Optical algorithms at satellite wavelengths for total suspended matter in tropical coastal waters. Sensors 8(7):4165–4185. doi:10.3390/s8074165

Pais-Barbosa J, Veloso-Gomes F, Taveira-Pinto F (2009) Portuguese northwest beach classification using aerial photographs and GIS tools. J Coastal Res SI 56:1552–1556

Pal NR, Pal SK (1993) A review on image segmentation techniques. Pattern Recognit 26(9):1277–1294. doi:10.1016/0031-3203(93)90135-J

Rahman MR, Saha SK (2008) Multi-resolution segmentation for object-based classification and accuracy assessment of land use/land cover classification using remotely sensed data. J Indian Soc Remote Sens 36(2):189–201. doi:10.1007/s12524-008-0020-4

R Core Team (2013) R: a language and environment for statistical computing, R Foundation for Statistical Computing, Vienna, Austria. http://www.R-project.org/. Accessed 20 July 2015

Ripley B, Venables W (2014) Nnnet: feed-forward neural networks and multinomial loglinear models. R package version 7.3–8. In: CRAN repository. Available via http://cran.r-project.org/web/packages/nnet/nnet.pdf. Accessed 19 Feb 2014

Ritchie JC, McHenry JR, Schiebe FR, Wilson RB (1974) The relationship of reflected solar radiation and the concentration of sediment in the surface water of reservoirs. In: Ritchie JC (ed) Remote sensing of earth resources, vol III. University of Tennessee Space Institute, Tullahoma, pp 57–72

Rodríguez-Guzmán V, Gilbes-Santaella F (2009) Estimating total suspended sediments in tropical open bay conditions using MODIS. In: Chen S, Li Q (eds) Proceeding of IMCAS'09 proceedings of the 8th WSEAS international conference on instrumentation, measurement, circuits and systems. China Jiliang University & Zhejiang University of Technology, China, pp 20–22

Rodríguez-Martín R, Rodríguez-Santalla I (2013) Detection of submerged sand bars in the Ebro Delta using ASTER images. In: Huang H et al (eds) New frontiers in engineering geology and the environment, vol 9. Springer, Berlin, pp 103–106

Roy DP, Wulder MA, Loveland TR, Woodcock CE, Allen RG, Anderson MC, Helder D, Irons JR, Johnson DM, Kennedy R, Scambos TA, Schaaf CB, Schott JR, Sheng Y, Vermote EF, Belward AS, Bindschadler R, Cohen WB, Gao F, Hipple JD, Hostert P, Huntington J, Justice CO, Kilic A, Kovalskyy V, Lee ZP, Lymburner L, Masek JG, McCorkel J, Shuai Y, Trezza R, Vogelmann J, Wynne RH, Zhu Z (2014) Landsat-8: science and product vision for terrestrial global change research. Remote Sens Environ 145:154–172. doi:10.1016/j.rse.2014.02.001

Ruddick K, De Cauwer V, Park Y, Becu G, De Blauwe J-P, De Vreker E, Deschamps P-Y, Knockaert M, Nechad B, Pollentier A, Roose P, Saudemont D, Van Tuyckom D (2003) Preliminary validation of meris water prod-

ucts for Belgian coastal waters. In: Proceedings of Envisat validation workshop, ESA SP-531, Frascati, Mar 2003

Rudorff ND, Kampel M, de Rezende CE (2011) Spectral mapping of the Paraíba do Sul River plume (Brazil) using multitemporal Landsat images. J Appl Remote Sens 5(1):053550. doi:10.1117/1.3630220

Sanjeevi S (1996) Morphology of dunes of the Coromandel coast of Tamil Nadu: a satellite data based approach for coastal landuse planning. Landsc Urban Plan 34(3–4):189–195. doi:10.1016/0169-2046(95)00233-2

Saran S, Sterk G, Kumar S (2009) Optimal land use/land cover classification using remote sensing imagery for hydrological modeling in a Himalayan watershed. J Appl Remote Sens 3(1):033551. doi:10.1117/1.3253618

Satellite Imaging Corporation (2015) Satellite sensors. Available via http://www.satimagingcorp.com/satellite-sensors/. Accessed 05 July 2015

Schiewe J (2002) Segmentation of high-resolution remotely sensed data – concepts, applications and problems. In: Armenakis C, Lee YC (eds) Joint ISPRS commission IV symposium: geospatial theory, processing and applications, Ottawa, 9–12 July 2002. ISPRS Archives, vol XXXIV part 4, p 6

Schiller H, Doerffer R (2005) Improved determination of coastal water constituent concentration from MERIS data. IEEE Trans Geosci Remote Sens 43(7):1585–1591. doi:10.1109/TGRS.2005.848410

Shi W, Wang M (2009) Satellite observations of flood-driven Mississippi River plume in the spring of 2008. Geophys Res Lett 36(7):L07607. doi:10.1029/2009GL037210

Short AD (1991) Macro-meso tidal beach morphodynamics: an overview. J Coastal Res 7(2):417–436

Short AD (1999) Beach and shoreface morphodynamics. Wiley, England

Short AD (2006) Australian beach systems – nature and distribution. J Coastal Res 22(1):11–27, doi:http://dx.doi.org/10.2112/05A-0002.1

Short AD (2012) Beach morphodynamics in Australia 1970s–2010. Geogr Res 50(2):141–153. doi:10.1111/j.1745-5871.2012.00760.x

Shridhar DJ, Alvarinho JL (2013) Very high-resolution satellite data for improved land cover extraction of Larsemann Hills, Eastern Antarctica. J Appl Remote Sens 7(1):073460. doi:10.1117/1.JRS.7.073460

Silveira M, Heleno S (2009) Separation between water and land in SAR images using region-based level sets. IEEE Geosci Remote Sens 6(3):471–475. doi:10.1109/LGRS.2009.2017283

Son YB, Gardner WD, Richardson MJ, Ishizaka J, Ryu JH, Kim S-H, Lee SH (2012) Tracing offshore low-salinity plumes in the Northeastern Gulf of Mexico during the summer season by use of multispectral remote-sensing data. J Oceanogr 68(5):743–760. doi:10.1007/s10872-012-0131-y

Song XF, Duan Z, Jiang XG (2012) Comparison of artificial neural networks and support vector machine classifiers for land cover classification in Northern China using a SPOT-5 HRG image. Int J Remote Sens 33(10):3301–3320. doi:10.1080/01431161.2011.568531

Sousa A, García-Murillo P (2003) Changes in the Wetlands of Andalusia (Doñana Natural Park, SW Spain) at the end of the Little Ice Age. Clim Change 58(1–2):193–217. doi:10.1023/A:1023421202961

Sousa A, García-Murillo P, Sahin S, Morales J, García-Barrón L (2010) Wetland place names as indicators of manifestations of recent climate change in SW Spain (Doñana Natural Park). Clim Change 100(3–4):525–557. doi:10.1007/s10584-009-9794-9

Sousa A, Morales J, García-Barrón L, García-Murillo P (2013) Changes in the Erica ciliaris Loefl. ex L. peat bogs of southwestern Europe from the 17th to the 20th centuries AD. The Holocene 23(2):255–269. doi:10.1177/0959683612455545

Story M, Congalton RG (1986) Accuracy assessment: a user's perspective. Photogramm Eng Remote Sens 52(3):397–399

Tang S, Larouche P, Niemi A, Michel C (2013) Regional algorithms for remote-sensing estimates of total suspended matter in the Beaufort Sea. Int J Remote Sens 34(19):6562–6576. doi:10.1080/01431161.2013.804222

Teodoro AC (2015) Applicability of data mining algorithms in the identification of beach features/patterns on high-resolution satellite data. J Appl Remote Sens 9(1):095095. doi:10.1117/1.JRS.9.095095

Teodoro A, Almeida H (2011) Spatio-temporal variability analysis of the Douro River plume through MERIS data for one hydrological year. In: Neale MU, Maltese A (eds) Proceeding of the conference on remote sensing for agriculture, ecosystems, and hydrology XIII/18th international symposium on remote sensing, vol 8174, 10.1117/12.897519, 81741N, Prague, 19–21 Sept 2011

Teodoro AC, Gonçalves H (2011) Extraction of estuarine/coastal environmental bodies from satellite data through image segmentation techniques. In: Pei-Gee Ho (ed) Image segmentation. InTech, pp 435–458. ISBN: 978-953-307-228-9. doi:10.5772/14672

Teodoro AC, Gonçalves H (2012) A semi-automatic approach for the extraction of sandy bodies (Sand Spits) from IKONOS-2 data. IEEE J Sel Top Appl 5(2):634–642. doi:10.1109/JSTARS.2011.2181339

Teodoro AC, Veloso-Gomes F (2007) Quantification of the total suspended matter concentration around the sea breaking zone from in situ measurements and terra/aster data. Mar Georesour Geotechnol 25(2):67–80. doi:10.1080/10641190701334164

Teodoro AC, Marçal ARS, Veloso-Gomes F (2007a) Correlation analysis of water wave reflectance and local TSM concentrations in the breaking zone, using remote sensing techniques. J Coastal Res 23(6):1491–1497, doi:http://dx.doi.org/10.2112/05-0482.1

Teodoro AC, Veloso-Gomes F, Gonçalves H (2007b) Retrieving TSM concentration from multispectral satellite data by multiple regression and artificial neural

networks. IEEE T Geosci Remote 45(5):1342–1350. doi:10.1109/TGRS.2007.893566

Teodoro AC, Veloso-Gomes F, Gonçalves H (2008) Statistical techniques for correlating total suspended matter concentration with seawater reflectance using multispectral satellite data. J Coastal Res 24(4A):40–49, doi:http://dx.doi.org/10.2112/06-0770.1

Teodoro AC, Gonçalves H, Veloso-Gomes F, Gonçalves JA (2009a) Modelling of the Douro river plume size, obtained through image segmentation of MERIS data. IEEE Geosci Remote Sens 6(1):87–91. doi:10.1109/LGRS.2008.2008446

Teodoro AC, Pais-Barbosa J, Veloso-Gomes F, Taveira-Pinto F (2009b) Beach hydromorphological classification through image classification techniques applied to remotely sensed data. Michel U, Civco DL (eds) Remote sensing for environmental monitoring, GIS applications, and geology IX. Proceedings of SPIE, vol 7478, 747827, Berlin, 31Aug 2009

Teodoro AC, Pais-Barbosa J, Veloso-Gomes F, Taveira-Pinto F (2009c) Evolution of beach hydromorphological behaviour and classification using image classification techniques. J Coastal Res SI 56(2):1607–1611

Teodoro AC, Gonçalves H, Pais-Barbosa J, Veloso-Gomes F, Taveira-Pinto F (2010) Identification of beach features/patterns through artificial neural networks techniques using IKONOS data. In: Wagner W, Székely B (eds) ISPRS TC VII symposium – 100 years ISPRS, Vienna, 5–7 Jul 2010. ISPRS Archives, vol XXXVIII, Part 7B, pp 574–579

Teodoro AC, Pais-Barbosa J, Gonçalves H, Veloso-Gomes F, Taveira-Pinto F (2011a) Extraction of Cabedelo sand spit area (Douro estuary) from satellite images through image processing techniques. J Coastal Res SI 64:1740–1744

Teodoro AC, Pais-Barbosa J, Gonçalves H, Veloso-Gomes F, Taveira-Pinto F (2011b) Identification of beach features/patterns through image classification techniques applied to remotely sensed data. Int J Remote Sens 32(22):7399–7422. doi:10.1080/01431161.2010.523729

Teodoro AC, Pais-Barbosa J, Gonçalves H, Veloso-Gomes F, Taveira-Pinto F (2011c) Beach hydromorphological analysis through remote sensing. J Coastal Res SI 61:44–51, doi:http://dx.doi.org/10.2112/SI61-001.55

Teodoro AC, Ferreira D, Gonçalves H (2013) The use of decision trees in the classification of beach forms/patterns on IKONOS-2 data. In: Michel U, Civco DL, Schulz K, Ehlers M, Nikolakopoulos KG (eds) Earth resources and environmental remote sensing/GIS applications IV. Proceedings of SPIE, vol 8893, SPIE, Bellingham, WA 2013, 88930N, Dresden, 23–25 Sept 2013

Therneau TM, Atkinson EJ (1997) An introduction to recursive partitioning using the rpart routines. Technical report 61, section of biostatistics, Mayo Clinic, Rochester

Turner W, Spector S, Gardiner N, Fladeland M, Sterling E, Steininger M (2003) Remote sensing for biodiversity science and conservation. Trends Ecol Evol 18(6):306–314. doi:10.1016/S0169-5347(03)00070-3

Urbański J (2009) Object based thematic mapping of coastal waters using MODIS satellite imagery. In: Proceedings of the 33rd international symposium on remote sensing of environment (ISRSE), Stresa, 4–8 May 2009

Vahtmäe E, Kutser T (2013) Classifying the Baltic Sea shallow water habitats using image-based and spectral library methods. Remote Sens 5(5):2451–2474. doi:10.3390/rs5052451

Valente AS, da Silva JCB (2009) On the observability of the fortnightly cycle of the Tagus estuary turbid plume using MODIS ocean colour images. J Mar Syst 75(1):131–137. doi:10.1016/j.jmarsys.2008.08.008

Vanden Borre J, Paelinckx D, Mücher CA, Kooistra L, Haest B, De Blust G, Schmidt AM (2011) Integrating remote sensing in Natura 2000 habitat monitoring: prospects on the way forward. J Nat Conserv 19(2):116–125. doi:10.1016/j.jnc.2010.07.003

Vanhellemont Q, Ruddick K (2014) Turbid wakes associated with offshore wind turbines observed with Landsat 8. Remote Sens Environ 145:105–115. doi:10.1016/j.rse.2014.01.009

Vantrepotte V, Loisel H, Mériaux X, Neukermans G, Dessailly D, Jamet C, Gensac E, Gardel A (2011) Seasonal and inter-annual (2002–2010) variability of the suspended particulate matter as retrieved from satellite ocean color sensor over the French Guiana coastal waters. J Coastal Res SI 64:1750–1754

Wang J (2009) Satellite remote sensing of suspended sediment concentrations in Turbid Rivers. Ph.D. dissertation, National University of Singapore

Wang YY, Li J (2008) Feature-selection ability of the decision-tree algorithm and the impact of feature-selection/extraction on decision-tree results based on hyperspectral data. Int J Remote Sens 29(10):2993–3010. doi:10.1080/01431160701442070

Warrick JA, Mertes LAK, Washburn L, Siegel DA (2004) Dispersal forcing of southern California river plumes, based on field and remote sensing observations. GeoMar Lett 24(1):46–52. doi:10.1007/s00367-003-0163-9

Warrick JA, DiGiacomo PM, Weisberg SB, Nezlin NP, Mengel M, Jones BH, Ohlmann JC, Washburn L, Terrill EJ, Farnsworth KL (2007) River plume patterns and dynamics within the Southern California Bight. Cont Shelf Res 27(19):2427–2448. doi:10.1016/j.csr.2007.06.015

Wassermann PD (1989) Neural computing theory and practice. Van Nostrand Reinhold Co, New York

Weih RC, Riggan ND (2010) Object-based classification vs. pixel-based classification: comparitive importance of multi-resolution imagery. In: Addink EA, Van Coillie FMB (eds) GEOBIA 2010: geographic object-based image analysis, Ghent, 29 June–2 July 2010. ISPRS Archives, vol XXXVIII-4/C7, p 6

Yang X (2009) Remote sensing and geospatial technologies for coastal ecosystem assessment and management. Springer, Berlin

Zhou W, Wang S, Zhou Y, Troy A (2006) Mapping the concentrations of total suspended matter in Lake Taihu, China, using Landsat-5 TM data. Int J Remote Sens 27(6):1177–1191. doi:10.1080/01431160500353825

Zhu W, Tian YQ, Yu Q, Becker BL (2013) Using Hyperion imagery to monitor the spatial and temporal distribution of colored dissolved organic matter in estuarine and coastal regions. Remote Sens Environ 134:342–354. doi:10.1016/j.rse.2013.03.009

Zhu W, Yu Q, Tian YQ, Becker BL, Zheng T, Carrick HJ (2014) An assessment of remote sensing algorithms for colored dissolved organic matter in complex freshwater environments. Remote Sens Environ 140:766–778. doi:10.1016/j.rse.2013.10.015

Author Queries

Chapter No.: 3 0002624057

Queries	Details Required	Author's Response
AU1	Please check captured abstract if correct.	
AU2	Please provide details for the citation "Rodríguez-Guzmán and Gilbes-Santaella (2009), Sousa et al. (2003), Frihy et al. (1997), and Canny (1996)" in the reference list.	
AU3	Please provide better quality of figure for Fig. 3.12	
AU4	Please cite Canny (1986), Frihy et al. (1998), Rodríguez-Guzmán et al. (2009), and Sousa and García-Murillo (2003) in the text.	